The Covalent Functionalization of Graphene on Substrates

Alejandro Criado, Michele Melchionna, Silvia Marchesan, and Maurizio Prato**

Keywords:
functionalization · graphene · graphene reactivity · nanotechnology

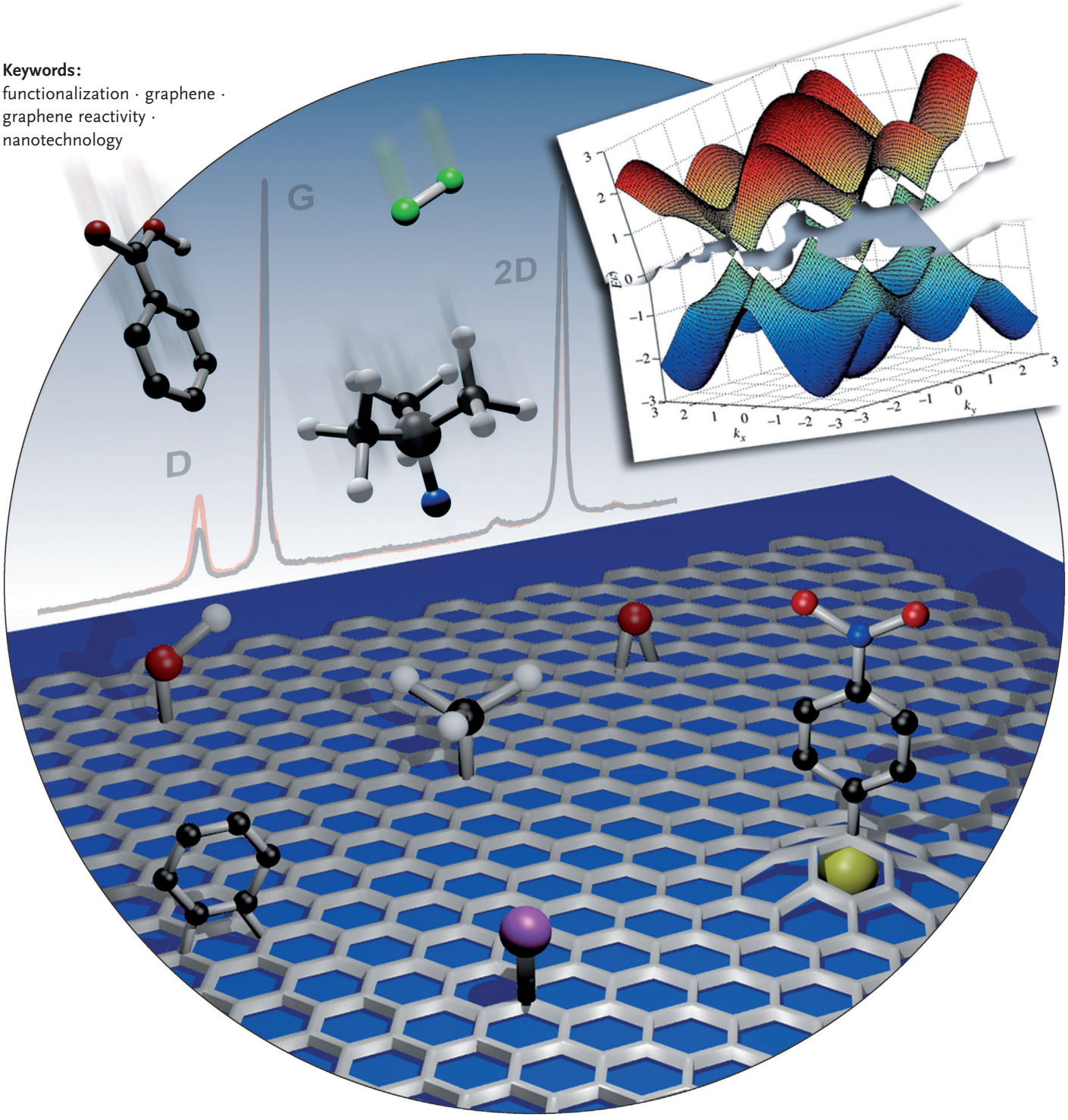

The utilization of grown or deposited graphene on solid substrates offers key benefits for functionalization processes, but especially to attain structures with a high level of control for electronics and "smart" materials. In this review, we will initially focus on the nature and properties of graphene on substrates, based on the method of preparation. We will then analyze the most relevant literature on the functionalization of graphene on substrates. In particular, we will comparatively discuss radical reactions, cycloadditions, halogenations, hydrogenations, and oxidations. We will especially address the question of how the reactivity of graphene is affected by its morphology (i.e., number of layers, defects, substrate, curvature, etc.).

From the Contents

1. Introduction

Graphene is a single atomic layer of sp^2-hybridized carbon atoms arranged in a honeycomb lattice with dimensions ranging from a few hundred nanometers to tens of micrometers.[1] Various different types of graphene can also be defined depending on the number of layers, layer dimension, and amount of oxygen present in the carbon structure.[2] The family of graphene-based materials exhibit a unique set of electronic, mechanical, and thermal properties.[3] Consequently, a wide variety of applications have been designed for graphene materials in sensing,[4] energy storage,[5] catalyst support,[6] supercapacitors,[7] and optoelectronic devices.[8] In most of these applications, graphene is supported on a substrate, because the production and handling of graphene in solution is technically challenging. This is due to the well-known graphene tendency toward restacking, and/or to the creation of defects that may negatively affect graphene properties. As a result, works on modified graphene in solution often include materials that are quite heterogeneous, and structurally not so well-defined. By contrast, the use of graphene on substrates has notable advantages, as it minimizes such issues. Indeed, the growth and deposition of graphene on substrates is an ideal approach to produce single monolayers of graphene of large dimensions, and similar structures that are suitably controlled for electronic use.[9]

Chemical functionalization of graphene on substrates is a topic of paramount importance, because it allows for the fine-tuning of the material's chemical and physical properties.[10] Graphene derivatization occurs through introduction of complex moieties, such as biomolecules, catalysts, polymers, or simply through addition of functional groups that can act as anchor sites for further modification. There are two main strategies to derivatize graphene on substrates: the covalent and the noncovalent approach. In particular, covalent functionalization is the most frequently employed route to modify carbon materials,[11] as it is easy to control and yields products of high stability over time and chemical conditions. This review focuses on the latest developments in covalent functionalization of graphene on substrates, including the newest findings in understanding factors affecting graphene reactivity, e.g., the production route to graphene-based materials (GBMs) and the substrates used. We will also analyze how graphene properties are affected by derivatization. Readers more generally interested in graphene modification routes (both covalent and noncovalent, on substrates or in solution) are referred to recent detailed accounts[12] and comprehensive reviews.[13]

In the remainder, we will apply the classification framework for GBMs as recently established within the European Union's GRAPHENE Flagship project, to ensure consistent and correct term use.[2] Since this review focuses on graphene on substrates, we will also adopt an analogous nomenclature to the one introduced by Koehler and Stark (Figure 1),[14] to clearly differentiate the type of substrate that supports graphene, the kind of GBM used, and the organic molecule to which graphene is covalently linked.

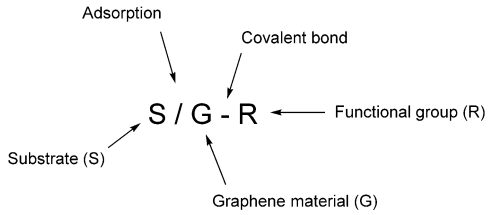

Figure 1. Nomenclature for functionalized graphene on a substrate.

2. Preparation of Graphene on Substrates

To understand and master reactivity toward covalent modification of graphene on substrates, it is imperative to first understand how the graphene properties depend on the graphene-on-substrate production route. There are numerous methods to obtain graphene on substrates of various quality. Both top-down[15] and bottom-up[16] approaches have been

[*] Dr. A. Criado, Dr. M. Melchionna, Dr. S. Marchesan, Prof. M. Prato
Department of Chemical and Pharmaceutical Sciences
University of Trieste
Piazzale Europa 1, 34127 Trieste (Italy)
E-mail: fcriado@units.it
prato@units.it

widely described.[9,17] Graphene on substrate is mainly produced by chemical vapor deposition (CVD) on metallic substrates (CVDG) or by epitaxial growth (EG). These bottom-up techniques produce high-quality monolayer and multilayer graphene films with a relatively small number of defects, thus making them useful for applications in electronic devices.

CVD is traditionally applied on metals, especially (poly- and monocrystalline) copper or nickel surfaces at high temperatures ($\approx$1000 °C), using methane or acetylene as carbon source under hydrogen flow, mainly to keep the catalyst in its metallic state.[16,18] In general, copper surfaces are superior substrates because they lead to monolayer graphene, whereas nickel is usually employed for preparing few-layer graphene. Recently, efforts have been devoted to optimize CVD synthesis by adopting more efficient heating methods or alternative low-temperature conditions. Examples include radio frequency magnetic inductive heating (RFCVD),[19] hydrogen-free processes such as plasma-enhanced CVD (PE-CVD),[20] rapid thermal CVD (RTCVD) at low temperature,[21] ambient-pressure CVD (APCVD),[22] or low-pressure CVD (LPCVD).[23]

EG is usually based on the thermal desorption of silicon from monocrystalline silicon carbide (0001).[24] In this type of substrate, there are two different surfaces, i.e., Si-terminated and C-terminated faces. Graphene that is grown from Si-faces is more adequate for high-speed electronic devices, given that it is a homogeneous few-layer graphene with high carrier mobility. In addition, the number of graphene layers may be determined through temperature control. By contrast, graphene grown on C-faces is heterogeneous and multilayered because of the higher reactivity of the surface. The main disadvantages of this production method are that SiC is an expensive substrate, and that EG is difficult to transfer onto other substrates. Alternatively, other monocrystalline metal substrates can be used in CVD to yield EG.[22b,25] However, the materials employed are costly, and thus limited by their small dimensions, hindering the scale-up of graphene production.

Graphene prepared by all the methods described above is viable for the production of graphene-based electronic devices. However, the corresponding substrates are typically too expensive, or simply unsuitable for such use. For this reason, transfer processes of graphene onto more appropriate substrates is often required, e.g., through peeling[26] or etching by oxygen plasma[27] and catalytic metals.[16,28]

Graphene on substrates can also be produced by top-down physical and chemical exfoliation of bulk graphite,[15b] followed by graphene film deposition. Several methods have been developed such as electrochemical exfoliation,[29] liquid phase exfoliation,[30] graphite intercalation,[31] chemical oxidation followed by reduction,[32] and mechanical cleavage.[33] The advantage of these routes is that exfoliated graphene (XG) suspensions can be conveniently deposited on a substrate of choice. This can be achieved in several ways, for example, by peeling,[1a] covalent attachment,[34] spraying,[35] drop-casting,[36] spin-coating,[37] and dip-coating.[38] These methods are cost-effective, versatile, high-yield, and allow for large-scale output. However, size and thickness of the obtained few-layer graphene materials are of limited homogeneity.

Alejandro Criado received his B.S. degree in chemistry, followed by his PhD in organic chemistry with Professor Enrique Guitián at the University of Santiago de Compostela. He is currently a postdoctoral fellow at the University of Trieste in the carbon nanotechnology group of Professor Maurizio Prato. His research focuses on new approaches for the organic functionalization of carbon nanostructures along with the development of graphene-based sensors.

Silvia Marchesan obtained her PhD in chemistry at The University of Edinburgh in 2008. She worked as honorary researcher at University College London, and did her postdoctoral research first at the University of Helsinki, and then as a joint fellow between The Commonwealth Scientific and Industrial Research Organization (CSIRO) and Monash University, in Melbourne. She returned to Italy in 2013 to join the University of Trieste as Assistant Professor. Her main interests lie at the interface between nanomaterials and biology.

Michele Melchionna completed his PhD in chemistry at the University of Edinburgh in 2007. He then carried out postdoctoral research both in academia (University of Helsinki, Finland, and Palacky University, Czech Republic) and industry (Advanced Molecular Technologies, Australia) focusing on organic synthesis and catalysis. He currently holds a position as senior postdoctoral fellow at the University of Trieste, working on carbon-nanostructure-based catalysts for energy applications.

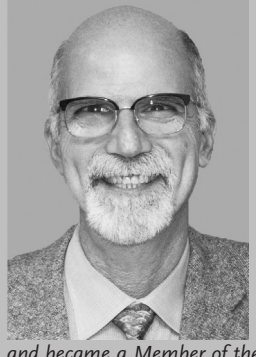

Maurizio Prato graduated in Padova, Italy, where he was appointed Assistant Professor in 1983. He moved to Trieste as an Associate Professor in 1992, and then was promoted to Full Professor in 2000. He spent sabbatical terms at Yale University and at the University of California, Santa Barbara. He was Visiting Professor at Ecole Normale Supérieure Paris (2001), the University of Namur, Belgium (2010), and the University of Strasbourg (2014). He was the recipient of an ERC Advanced Research Grant, European Research Council (2008) and became a Member of the National Academy of Sciences (Accademia Nazionale dei Lincei) in 2010.

3. Covalent Functionalization

Within the family of carbon nanomaterials, such as fullerenes, carbon nanotubes, and carbon nanohorns, graphene shows the lowest reactivity because of the lower curvature in the basal plane.[39] Indeed, according to π-orbital axis vector (POAV) analysis, the carbon atoms that are located in highly curved surfaces show higher chemical reactivity, due to decreased electronic delocalization.[40] However, graphene is not a totally flat material, as it exhibits intrinsic out-of-plane deformations.[41] Accordingly, carbon atoms at corrugated parts, edges, and defects are more reactive than those in the basal plane.[39,42]

Many efforts have been made for the functionalization of GBMs in both covalent and noncovalent fashion.[12,13] Covalent modification is the most studied form of graphene functionalization. This is due to the fact that covalent functionalization causes the most significant changes to the electrical properties of graphene, such as the opening of zero bandgap, and allows for the introduction of a wide variety of functional groups on the graphene surface. For this reason, the direct modification of graphene on substrates is very attractive. It is worth noting that generalizations in this respect can be misleading, because the outcome of graphene derivatization is strongly influenced by a number of factors that should not be neglected (e.g., graphene shape). Therefore, in this Review, we will clearly distinguish among the different graphene types on substrate materials.

Covalent functionalization of graphene on substrates is carried out by using diverse protocols. Reaction conditions are usually determined by the type of functionalization. In general, commonly employed procedures consist of placing graphene on substrates in contact with reagents in solution, of drop-casting the reactive solution onto graphene on substrates, of flowing-gas reagents, or of using plasma phases.

The extent of graphene functionalization can be roughly determined by Raman spectroscopy. An increase of the D-band with respect to the G-band is generally attributed to an increase of the defects, also associated with functionalization. Therefore, the intensity ratio I_D/I_G between D-band and G-band can be considered a measure of the functionalization degree.

In the following paragraphs, we will analyze the various approaches toward functionalization of graphene on substrates based on reaction classes, including the characteristic advantages/disadvantages of each process (Table 1). Covalent derivatization routes are grouped in: radical reactions, cycloadditions, and single-atom introductions.

3.1. Radical Reactions

A very popular approach for the functionalization of graphene surfaces is the addition of aryl radicals generated from the reduction of diazonium salts. The as-formed radical then attacks the sp^2-hybridized graphene framework, forming new C(sp^3)–aryl bonds.[43] This strategy leads to high functionalization degrees and has also the advantage of being tolerant of a variety of conditions (e.g., the solvent used). In addition, the reactive diazonium salts can be conveniently generated in situ in one-pot reactions. However, the high efficiency of the generation of radical species is a double-edged sword, as it often translates into poor control of the functionalization. In fact, it has been shown that the diazo coupling route often leads to not-well-defined chemical structures attached on the graphene surface. Local oligomer formation can be due to the reaction of excess aryl radicals with graphene-attached aryl groups (Figure 2a).[44] Growth of

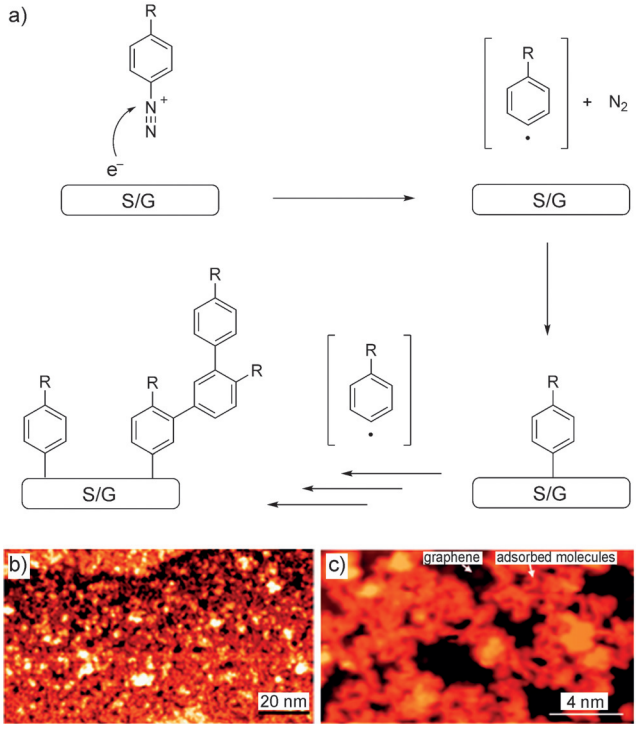

Figure 2. a) Aryl diazonium coupling on S/G. b,c) STM images of SiC/EG-(*p*NO_2Ph) at low (b) and high (c) magnification showing the presence of oligomers. Reproduced from Ref. [44], Copyright 2012 American Chemical Society.

aryl layers is also possible through aromatic homolytic substitution with aryl groups (or biaryl coupling), thus creating aryl oligomers prior to their addition onto graphene.[45] Evidence of aryl oligomers has been provided by scanning tunneling microscope (STM) imaging, which revealed emergence of an irregular surface upon diazo-coupling on graphene (Figure 2b,c). Efforts to control this process and to eliminate the formation of the resulting undesired organic insulating layer on graphene would be very valuable for the implementation of this route in conductive devices.[46]

The chemical properties of graphene on a substrate depend strongly on the graphene shape, number of layers, and nature of the substrate, as previously mentioned. This dependence is clearly reflected in diazonium chemistry. The substrate has a marked influence on reactivity.[47] CVD-grown graphene was transferred onto a variety of substrates using a polymer-mediated transfer method, and it was subsequently functionalized with 4-nitrophenyl diazonium tetrafluorobo-

rate (Figure 3).[47a] The tested substrates were: a single-crystal wafer of α-Al_2O_3 (c-face sapphire); and three substrates of SiO_2 on a silicon wafer, namely: bare SiO_2, and SiO_2 coated either with a self-assembled monolayer of octadecyltrichlorosilane (OTS) or a mechanically exfoliated flake of single-crystal hexagonal boron nitride (hBN). Functionalization was assessed by Raman spectroscopic mapping, which revealed a higher I_D/I_G ratio for graphene on SiO_2 and Al_2O_3 relative to graphene on hBN- and OTS-treated substrates, indicating lower reactivity for hydrophobic substrates. Contact-angle

Table 1: Main covalent functionalization processes of graphene on substrates.

Reaction	Advantages	Disadvantages	Type of graphene	Functionalization level (Raman I_D/I_G)	Ref.
Diazo coupling	high functionalization degree	potential oligomerization (poor control)	SiO_2/CVDG-NO_2Ph	0.86–0.88	[42a]
			Al_2O_3/CVDG-NO_2Ph	1.2	[47a]
			Si-OTS/CVDG-NO_2Ph	0.25	[47a]
			hBN/CVDG-NO_2Ph	0.25	[47a]
	tolerance for different experimental conditions (e.g., different solvents, preparation of precursors in situ or ex situ)		SiO_2/CVDG-NO_2Ph	1.5	[47a]
		heating and radical conditions not suitable to introduce sensitive biomolecules	SiO_2/XG-NO_2Ph	0.3–0.6	[47b]
			SiC/EG-NO_2Ph	2.6	[48a]
	wide applicability to introduce different chemical groups		Si/SLG-NO_2Ph	0.19-0.42[a]	[48b]
			Si/SLG-NO_2Ph (edges)	0.39–0.76[a]	[48b]
			Si/BLG-NO_2Ph	0.01	[48b]
		introduction of many defects	PDMS/XG-NO_2Ph	0.37–0.56[b]	[48d]
	possibility of performance in water or dry conditions (green conditions)		PDMS/XG-BrPh	0.20–0.57[b]	[48d]
			PDMS/CVDG-NO_2Ph	0.35–0.82[b]	[49a]
			PDMS/CVDG-BrPh	0.2–0.6[b]	[49a]
			PDMS/CVDG-MeOPh	0.25-0.85[b]	[49a]
Polymerization	devoid of defect introduction, preserves graphene chemical structure	coverage of large areas of graphene surface, which becomes inaccessible for further chemistry	Cu/CVDG-polystyrene	0.0–0.6[c]	[54]
	rapid method to introduce large molecules	impossibility to monitor the degree of functionalization by Raman[c]			
	ease of fine-tuning the material morphology due to the polymer (e.g., thermoresponsiveness; brush to mushroom morphology transitions)	impossibility to functionalize high-quality graphene that is virtually devoid of defects[c]	SiC/EG-polystyrene	0.0–0.6[c]	[54]
Cycloaddition	high level of control of functionalization degree and defects	reversibility (if undesired)	Si/XHOPG-DA-MA[d]	0.0–0.63[e]	[57]
			SiC/EG-DA-MA[d]	0.3	[57]
	wide applicability to introduce different chemical groups		Si/XSLG-DA-TCNE[d]	>1	[57]
		heating conditions not suitable to introduce sensitive biomolecules	Si/XHOPG-DA-TCNE[d]	0.22	[57]
			Si/XHOPG-DA-DMBD[d]	0.06–0.38[e]	[57]
	Reversibility (if desired)		SiC/EG-DA-DMBD[d]	0.0–0.5[e]	[57]
			Si/XHOPG-DA-MeA[d]	0.09–1.88[e]	[57]
Introduction of single atoms	ability to achieve electrical insulation		Si/CVDG-Cl	1.3–2.1	[74b]
	high levels of functionalization are possible		Si/XG-Cl	1.3–2.1	[74b]
	very fast reactions	aggressive conditions not suitable to introduce sensitive biomolecules or labile groups	Cu/CVDG-F	1[g]	[74a]
	possibility of performance in dry conditions		Cu/XG-F	1[g]	[74a]
		specific apparatus and expertise required (e.g., plasma generator, use of toxic gas-reactants)	SiO_2/XGNR-F[f]	1.5	[74e]
	possibility of using halogens as leaving groups to introduce sensitive biomolecules or other chemical		SiO_2/XGNR-Cl[f]	2.5	[74e]
		halogenation is efficient only on monolayer graphene	SiO_2/XGNR-H[f]	3.2	[74e]

[a] Functionalization degree depends on experimental conditions (e.g., temperature, reactant concentration). [b] Functionalization degree depends on strain applied to the flexible substrate, thus introducing wrinkles on graphene. [c] Reaction occurs on existing defect sites, thus I_D/I_G does not change upon functionalization. [d] DA = Diels–Alder reaction; TCNE = tetracyanoethylene; MA = maleic anhydride; DMBD = 2,3-dimethoxy-1.3-butadiene; MeA = 9-methyl-anthracene. [e] Functionalization degree depends on temperature, which can also revert the reaction. [f] GNR = graphene nanoribbons. [g] CVDG reacts faster than XG.

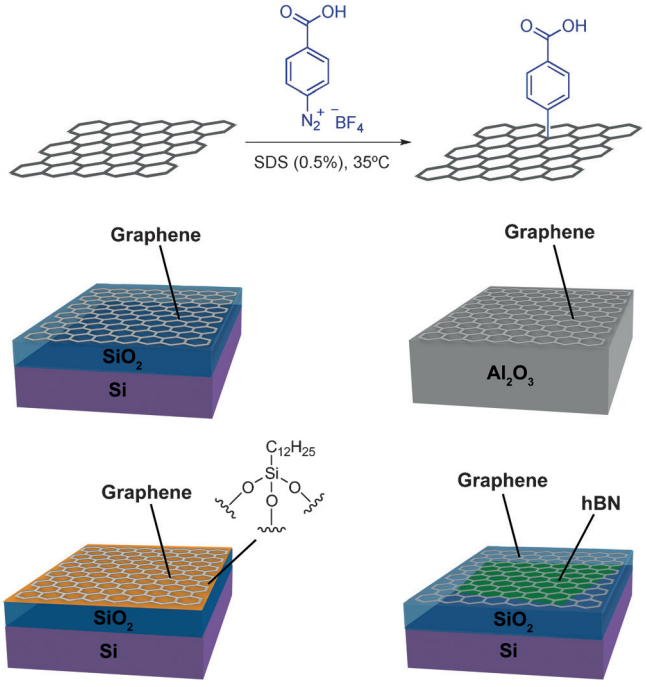

Figure 3. Scheme of diazonium coupling onto graphene (top) and the different materials used as substrates to support graphene. SDS = Sodium dodecyl sulfate. Based on Ref. [47a].

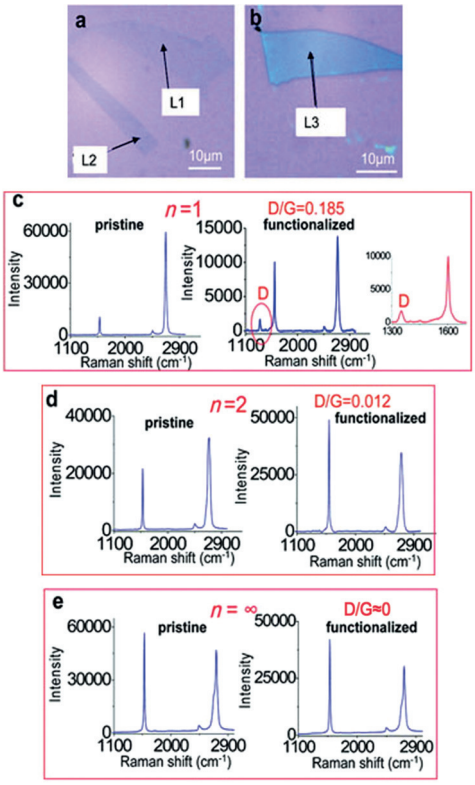

Figure 4. Optical images of a) SLG (L1), BLG (L2), and b) MLG (L3). Raman spectra of functionalized c) SLG, d) BLG, and e) MLG on silicon wafer. D = disorder-induced mode, G = E_{2g} vibrational mode of sp^2 bonded carbon atoms. Reprinted from Ref. [48b], Copyright 2010 American Chemical Society.

measurements were in agreement with these results, as they confirmed an inverse correlation between hydrophobicity and chemical reactivity. The higher reactivity observed for hydrophilic substrates (i.e., SiO_2 and Al_2O_3) was attributed to higher electron-hole fluctuations in the Fermi level of graphene produced by charged impurities or polar adsorbates that were present on the underlying surfaces. Accordingly, the lower reactivity observed for hydrophobic surfaces was rationalized in terms of increased distance between such charged puddles and graphene (i.e., due to a bilayer in the case of hBN or the organic film for OTS-coated samples).

Strong evidence supported the dependence of chemical reactivity also on other key factors: the number of graphene layers and the site of graphene (i.e., bulk surface or edges).[48] Single-layer (SL), bilayer (BL), and multilayer (ML) graphene obtained from the micromechanical cleavage of bulk graphite were deposited on a silicon wafer and treated with 4-nitrophenyl diazonium tetrafluoroborate (Figure 4). Raman spectroscopy was employed to observe the difference in the reactivity of the different materials. SLG sheets proved to be almost ten times more reactive than BLG and MLG. In addition, the edges of SLG were at least twice more reactive than the bulk SLG sheets. There is an inverse relationship between reactivity and number of graphene layers owing to the presence of charged impurities on the substrate. Their net effect is an increase of the available electron density for electron transfer with the reactant, thus increasing the reactivity of graphene. This effect is more pronounced in a single layer relative to bi- or multilayer graphene, because of the increased distance in the latter between the charged puddles and the top layer of graphene that is available for functionalization. Besides, the higher reactivity of graphene edges relative to bulk graphene can be rationalized in terms of dangling bonds or an altered electronic structure at the edges, with symmetry-breaking of the honeycomb lattice as compared to the bulk region.

The chemical properties of graphene on a substrate also depend on the graphene shape. Recently, supported graphene was deformed through the participation of SiO_2 nanoparticles (NPs) to study its reactivity.[42a] CVD-grown graphene was transferred onto SiO_2 NPs, which were previously deposited on a silicon surface (Figure 5). SEM images of SiO_2/CVDG showed sites of different high curvature in the graphene structure. Next, samples were treated with the aryl radical precursor, 4-nitrophenyl diazonium tetrafluoroborate. Covalent functionalization was confirmed by Raman spectroscopy and XPS analysis. Spatial distribution of the aryl groups on the sample surface was evaluated using 2D micro-Raman mapping in the D-band region, revealing a higher increase of the I_D/I_G ratio in the deformed areas of the graphene surface. These results suggest that reaction of the aryl radicals is favored on the curved regions of graphene obtained thanks to the presence of the underlying NPs.

Deformations on graphene layers produced by mechanical strain can also tune the chemical reactivity of graphene.[49] To this end, a flexible substrate can be used, such as polydimethylsiloxane (PDMS).[49a] When a mechanical strain was applied by stretching the PDMS, a reversible,

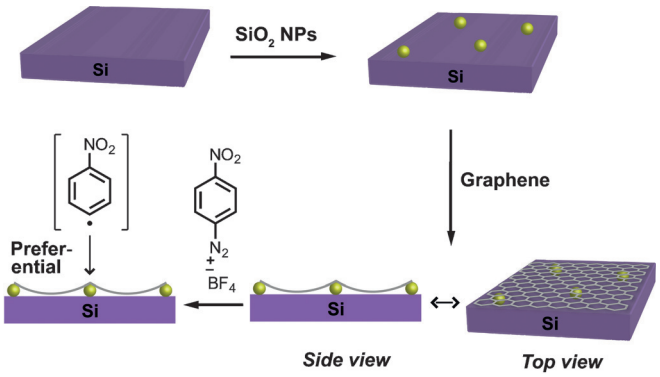

Figure 5. Selective functionalization on local curvatures of SiO_2/CVDG underlying gold NPs. Adapted from Ref. [42a], Copyright 2013 Royal Society of Chemistry.

non-homogeneous, and damage-free deformation was produced on the graphene structure. Next, graphene was functionalized with different aryl diazonium molecules such as 4-nitrophenyl diazonium, 4-bromophenyl diazonium, and 4-methoxyphenyl diazonium (4-MBD) salts, and compared with the corresponding functionalized PDMS/G substrates onto which a strain had not been applied. Strained graphene samples showed a reactivity that was up to ten times higher than that of the unstrained samples. Furthermore, mechanical strain enabled the functionalization with 4-nitrophenyl diazonium, which showed negligible reactivity on unstrained graphene (Figure 6). In addition, p- and n-type doping was achieved in the functionalized graphene depending on the used diazonium salt (p-dopant: 4-nitrophenyl group, n-dopant: 4-methoxyphenyl group). The doping was observed through the shift of the G and 2D bands in Raman spectroscopy, in particular, through up- or down-shifting to p- or n-type doping, respectively.

Aryl radicals are usually produced from aryl diazonium salts through thermal decomposition. Alternatively, electrochemical decomposition of diazonium salts under mild conditions is also possible.[50] Such an approach was used for the functionalization of large-area high-quality SLG obtained by CVD and transferred onto a layer of SiO_2 atop a silicon wafer. In the electrochemical process, the SiO_2/SLG was used as a working electrode in cyclic voltammetry (CV) experiments, through immersion in an acidic aqueous solution of the reactant, i.e., 4-nitrophenyl diazonium tetrafluoroborate. Remarkably, homogeneous functionalization was achieved, with an estimated nitrophenyl group coverage of 12.7–20.0 % of the graphene surface. Subsequently, the nitro groups were electrochemically reduced to amino groups. Eventually, the process, which includes radical addition followed by reduction, brought about the formation of C–C bonds on the graphene surface, where the n-type doping with amino groups might produce a bandgap opening in the graphene material and modulate its carrier mobility in a controllable way.

Organic groups introduced through diazonium chemistry on supported graphene can also be exploited to harness further modification with more complex molecular entities such as DNA, proteins, and antibodies for potential applications in biosensing or to immobilize biomolecules. In light of the selective reactivity of aryl radicals on hydrophilic surfaces as described above,[47a] CVD-grown graphene was transferred through reactivity imprint lithography onto a patterned substrate displaying both hydrophobic (OTS) and hydrophilic (SiO_2) areas. Next, it was functionalized with 4-carboxyphenyldiazonium tetrafluoroborate (Figure 7). The introduction of the carboxyphenyl moieties was confirmed by attenuated total reflectance infrared (ATR-IR) analysis. Attachment of carboxyphenyl groups on graphene allowed to create amide bonds with N_α,N_α-bis(carboxymethyl)-L-lysine hydrate leading to the formation of nitrilotriacetic acid (NTA) units that could chelate nickel(II). In this way, upon addition of $NiCl_2$, functionalized graphene displayed NTA-Ni complexes that were used as anchors for polyhistidine (His)-tagged EGFP (enhanced GFP; GFP = green fluorescent protein), allowing for detection by confocal fluorescence microscopy.

In addition to the diazonium salt chemistry, an alternative phenyl radical addition method is the photochemical approach, using benzoyl peroxide as phenyl radical precursor, under laser illumination (Figure 8a).[51] The reaction was performed with mechanically exfoliated graphene on a silicon-oxide-coated silicon wafer (SiO_2/G). Covalent function-

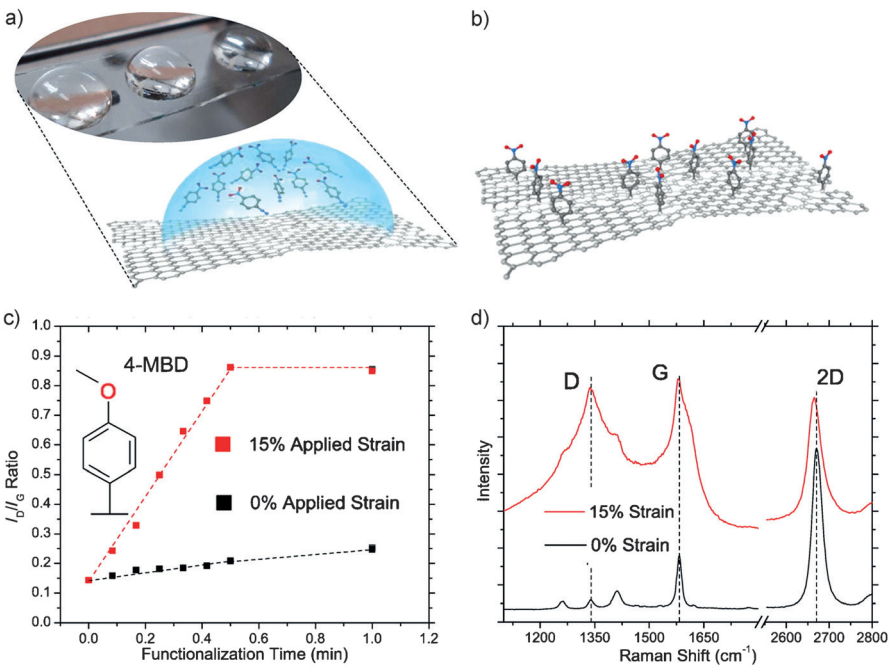

Figure 6. a,b) Schematic functionalization of strained PDMS/G with 4-MBD. c,d) Raman data of 15 % and 0 % strained PDMS/G-(*p*-CH_3Ph). Reproduced from Ref. [49a], Copyright 2013 American Chemical Society.

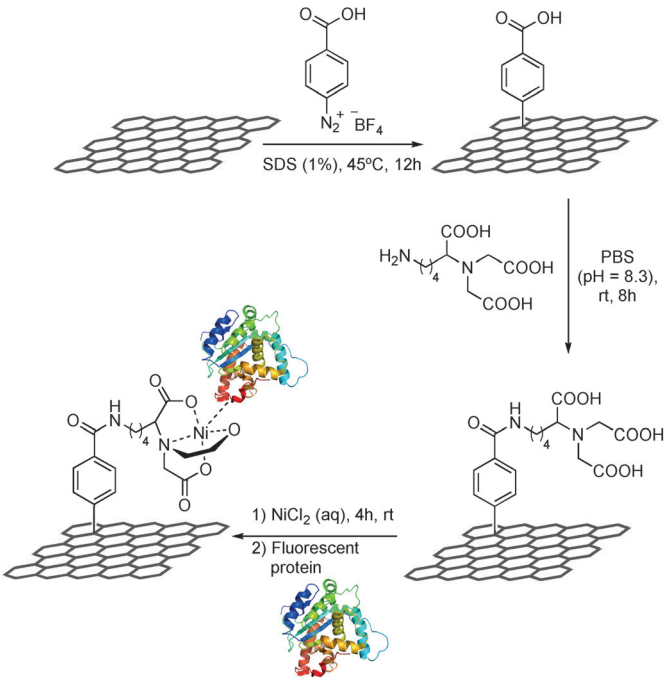

Figure 7. Anchoring of fluorescent protein onto functionalized CVD-G on OTS-patterned SiO_2. PBS = phosphate buffered saline. Based on Ref. [47a].

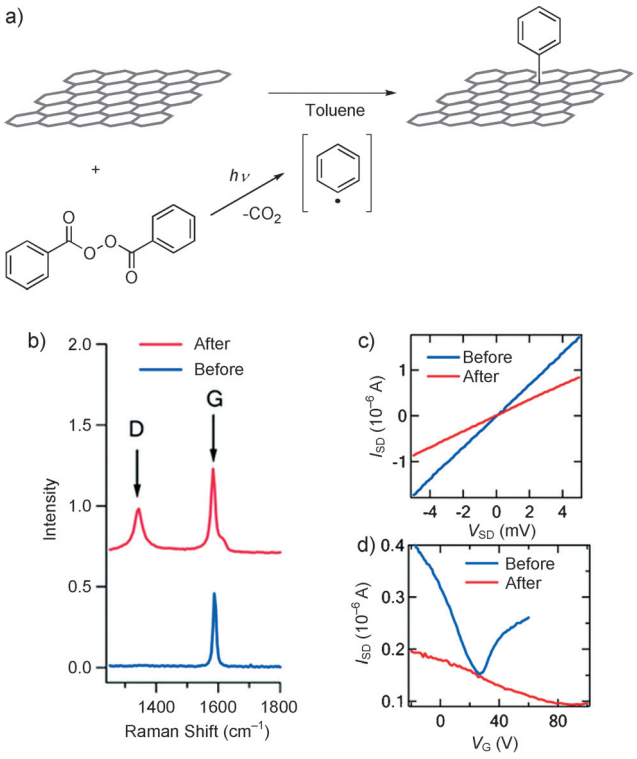

Figure 8. a) Radical functionalization of graphene with phenyl groups by photochemical decomposition of benzoyl peroxide in a drop-cast solution on SiO_2/G. b) Raman spectra, c) output, and d) transfer properties (V_{SD} = 1 mV) of SiO_2/XG before (blue) and after (red) functionalization. Reproduced from Ref. [51], Copyright 2009 American Chemical Society.

alization was confirmed by the appearance of an intense D-band at 1343 cm^{-1} in the Raman spectra (Figure 8b). The proposed mechanism for this reaction initiates with an electron transfer from the photoexcited graphene onto the physisorbed benzoyl peroxide. Subsequently, the corresponding excited species decompose to the phenyl radical, which reacts with the sp^2 carbon atoms of the graphene basal planes. In addition, the reactivity of SLG and few-layer graphene (FLG) micro-scale films was compared, revealing a reactivity that was 14 times higher for the former relative to the latter. As the photochemical reaction was carried out in a graphene field-effect-transistor (GFET) device, the electrical conductivity notably decreased (50%) in agreement with the introduction of defect centers, and with the increment of the p-type doping level due to the physisorption of benzoyl peroxide on the graphene surface (Figure 8c,d).

Another way of generating phenyl radicals is the electrochemical decomposition of aryl iodonium salts.[52] SiC (0001)/EG was functionalized with trifluoromethylphenyl ($CF_3C_6H_4$-), which is a nonreactive, hydrophobic, electron-withdrawing group, obtained from a symmetric aryl iodonium salt (Figure 9). The applied reduction potential necessary for the decomposition of the corresponding iodonium salt was higher in comparison to their analogous diazonium salts. Importantly, the electrochemical anchoring of $CF_3C_6H_4$-moieties on EG increased the number of electronic states and the hydrophobicity of the graphene material due to the perpendicular orientation of the fluorine groups to the surface.

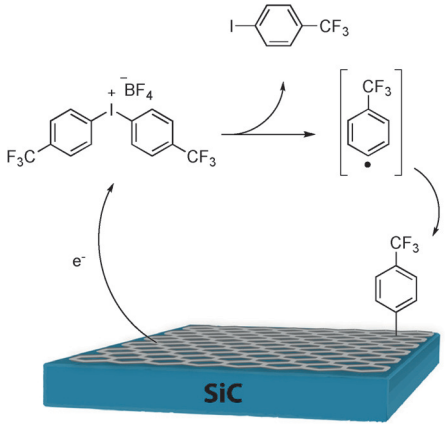

Figure 9. Proposed mechanism for radical functionalization of SiC/EG with trifluoromethylphenyl iodonium based on Ref. [52].

A particular case of radical functionalization of aromatic moieties on supported graphene is the reversible Kolbe reaction for the engineering of the band structure of graphene. The reaction consists of an electrochemical oxidation of carboxylate groups with subsequent addition of the corresponding carbon radicals.[53] In particular, the reversible electrochemical functionalization was based on the radical addition of 1-naphthylmethyl groups (Naph-CH_2-) to SiC/EG. The material was used as a working electrode in CV experiments, and thus it was immersed in a solution of 1-naphthylacetic acid. When an oxidation potential was applied,

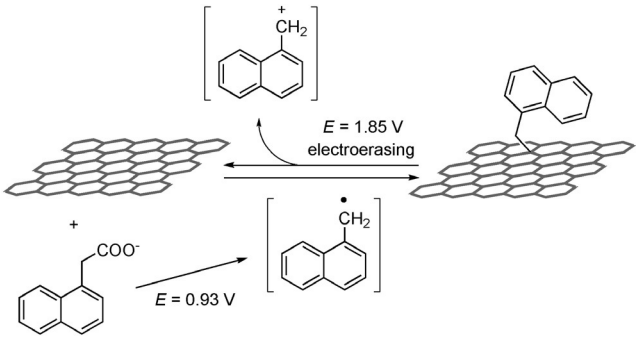

Figure 10. Reversible electrochemical production of SiC/EG-CH_2Naph.

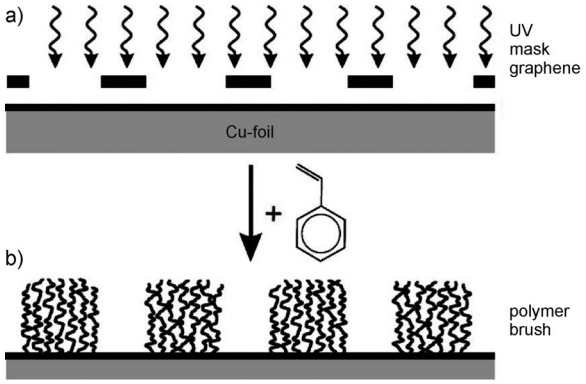

Figure 11. UV-assisted polymerization on single-layer Cu/CVDG. Reproduced from Ref. [54], Copyright 2011 American Chemical Society.

the oxidation of 1-naphthylacetate occurred (at 0.93 V vs. SCE), allowing for the chemical modification of graphene through the addition of 1-naphthylmethyl radicals (Figure 10). Complete functionalization of EG was easily achieved through the first scan (scan rate = 0.2 Vs^{-1}), as confirmed by the disappearance of the CV curve in successive cycles. SiC/EG-CH_2Naph showed a surface coverage by the introduced organic groups corresponding to 1×10^{-9} mol cm^{-2}. It is also worth noting that the complete passivation of the graphene surface was independent on the concentration of the radical precursor. A very interesting aspect is also that the whole process is completely reversible. Indeed, a complete defunctionalization was achieved through two cycles of oxidative CV (between 1 and 2.5 V vs. SCE). Remarkably, the resulting graphene material showed an electrical behavior similar to pristine EG, and its surface could be refunctionalized again under oxidative conditions.

Radical reactions on graphene are also considered a powerful chemical strategy to couple polymers to graphene surfaces. In situ covalent modification by photopolymerization with styrene was performed on SiC/EG and Cu/CVDG, to afford polystyrene brushes on the carbon material by using a mask (Figure 11).[54] Covalent attachment was confirmed by diffuse-reflectance infrared Fourier transform spectroscopy showing the characteristic vibrational modes of polystyrene groups. The UV-induced polymerization did not cause more defects in the conjugated graphene structure as confirmed by the unchanged I_D/I_G ratio in scanning Raman spectroscopy, and by the absence of variations in electrical transport measurements. These results suggest that photopolymerization took place at existing defects in the basal plane of graphene.

More recently, direct photopolymerization of CVDG transistors on a poly(methyl methacrylate) (PMMA) substrate was described to create a versatile scaffold for biosensing applications.[55] This functionalization onto GFET allowed for the detection of the neurotransmitter acetylcholine through two functionalities (Figure 12). To obtain the corresponding functionalities, two monomers were used, 1) *tert*-butyl methacrylate (*t*BMA) to introduce the carboxyl groups for the enzyme immobilization on graphene through a peptide bond, and 2) the *N,N*-dimethylaminoethyl methacrylate (DMAEMA) to incorporate pH-sensitive functional groups for the detection of byproducts of the enzymatic reaction. The functionalization was confirmed through XPS of the nitrogen 1s core level, which showed the corresponding peaks for the dimethylamino groups in the polymer. However, the covalent functionalization did not lead to the introduction of additional defects, as shown by the unchanged D-band in Raman spectra. Analogously to the polymerization method described above, also in this case the polymerization probably occurs at the existing defects in the graphene structure.

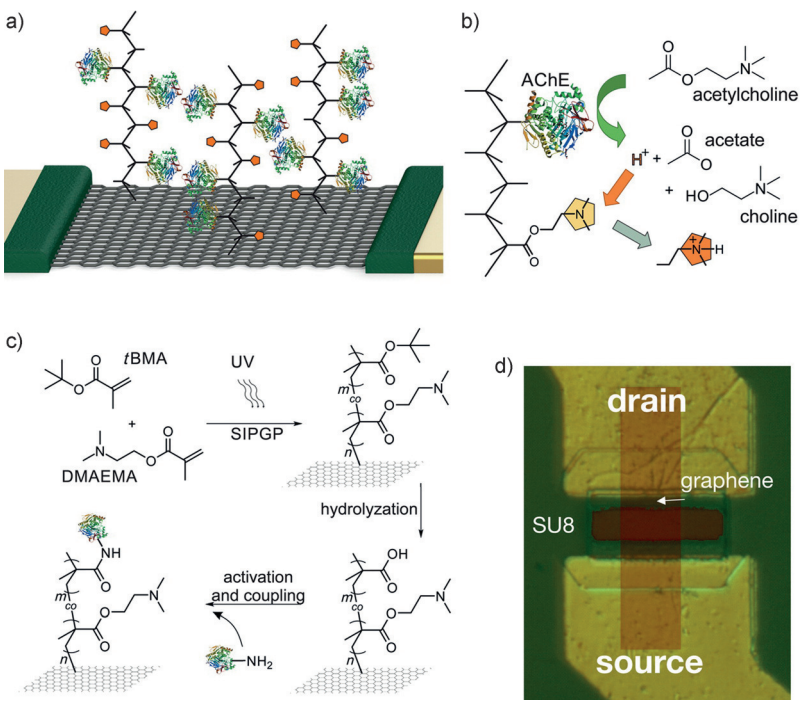

Figure 12. a) Schematic representation of GFET-biosensor based on photopolymerized PMMA/CVDG. b) Sensing mechanism of the biosensor. c) Formation of PMMA/CVDG functionalized with enzyme. d) Structure of GFET. Reprinted from Ref. [55], Copyright 2014 American Chemical Society.

3.2. Cycloaddition Reactions

The reversible modification of bandgap and conductivity of graphene on a substrate can usually be performed by Diels–Alder reactions. A [4+2] cycloaddition on graphene leads to changes of the hybridization of a pair of neighboring carbon atoms of the conjugated system from sp^2 to sp^3, resulting in an efficient opening of a bandgap on the carbon material. The [4+2] cycloadditions are governed by HOMO–LUMO interactions between diene and dienophile, and the energy gap between the orbitals is inversely proportional to reactivity. The Dirac point, i.e., the point at which the conduction and valence bands of graphene converge at the Fermi level allows graphene to behave both as a diene and as a dienophile in [4+2] cycloadditions.[56] Sarkar et al. have studied the reactivity of XG and EG on Si substrates in Diels–Alder reactions.[57] On one hand, the use of graphene as diene was performed with the activated dienophiles tetracyanoethylene (TCNE) and maleic anhydride (MA), and the reaction was monitored by Raman spectroscopy (Figure 13). The reaction of two graphene derivatives with TCNE at room temperature showed a significant increase of the I_D/I_G ratio that was reversed when the temperature was raised, confirming the reversibility of the process. In addition, the reaction of MA with Si/EG showed functionalization at 70 °C, whereas the retro-Diels–Alder product was observed at 150 °C. This covalent functionalization is very interesting for the reversible engineering of the graphene bandgap and conductivity for electronic applications.

On the other hand, the role of graphene on Si substrates as dienophile was investigated using 2,3-dimetoxy-1,3-butadiene. Graphene adducts obtained at 50 °C showed a higher level of functionalization than those obtained at higher temperatures due to their instability. The complete retro-Diels–Alder reaction was also in this case accomplished at 150 °C.

Graphene can also react as a diene in [4+2] cycloadditions with arynes. To date, several aryne cycloaddition reactions on different carbon nanomaterials have been described. Benzyne cycloaddition to fullerene, for instance, leads to [2+2] adducts.[58] However, for reactions performed on carbon nanotubes,[59] carbon nanohorns,[60] and graphene[61] there is no experimental evidence as yet about the exact structure of the adduct obtained. Several theoretical studies suggest that the kind of benzyne cycloaddition onto carbon nanotubes (i.e., either [4+2] or [2+2]) depends on different parameters, such as the kind of carbon nanotube used (i.e., number of walls, chirality, etc.) and its diameter.[59b,62] Similarly, it is reasonable to assume that both mechanistic pathways are possible for carbon nanohorns, in light of the different diameters which are simultaneously present in their conical nanostructures.[60] In the case of graphene, theoretical calculations argued that the reaction with benzyne on a graphene fragment of 4×4 unit cells occurred through [2+2] cycloaddition.[63] However, taking into account the characteristics of the graphene structure, including defects, roughness, and deformations, it appears reasonable to consider that both [4+2] and [2+2] cycloadditions can take place (Figure 14).

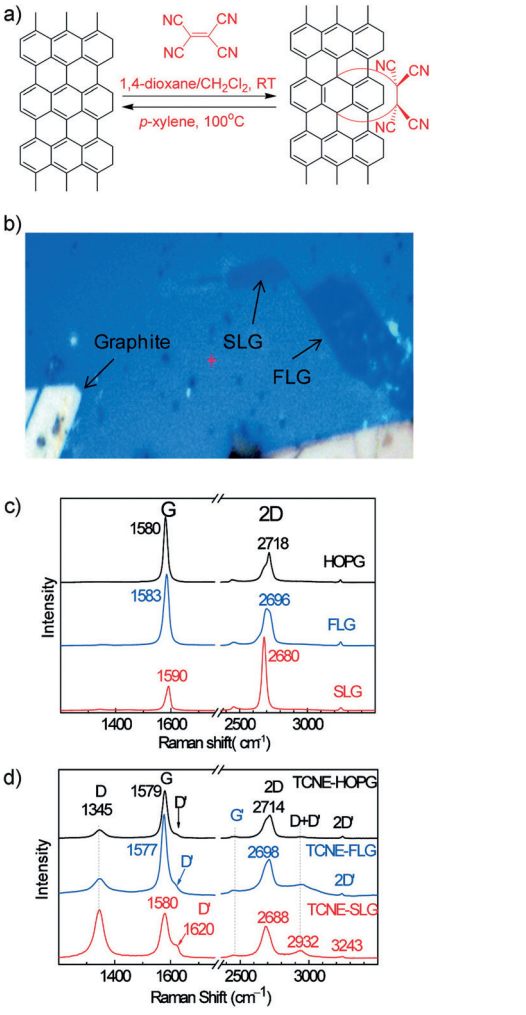

Figure 13. a) Diels–Alder reaction between SiO_2/XG and TCNE. b) Optical image showing a piece of graphite, SLG, and FLG in the sample of SiO_2/G. c,d) Raman spectra of graphite, FLG and SLG before (c) and after (d) Diels–Alder reaction. Reprinted from Ref. [57], Copyright 2011 American Chemical Society.

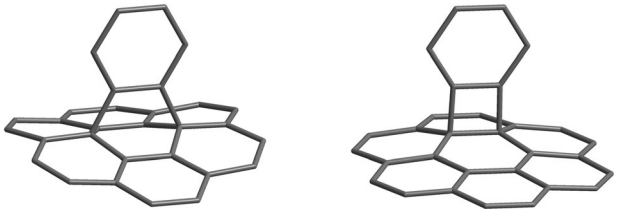

Figure 14. 3D simulation of the two possible adducts from a [4+2] (left) and [2+2] (right) cycloaddition of graphene with benzyne.

Aryne cycloaddition on supported graphene was carried out under mild conditions, immersing high-area Cu/G in a mixture of *o*-(trimethylsilyl)phenyl triflate (as benzyne precursor) and cesium fluoride, for several days (Figure 15 a).[64] Benzyne was generated by fluoride-induced elimination of trimethyl silyl (TMS) and triflate (OTf) from the corresponding precursors. The appearance of Raman and energy-dispersive X-ray (EDX) spectral signals confirmed the covalent modification of the carbon nanostructure (Fig-

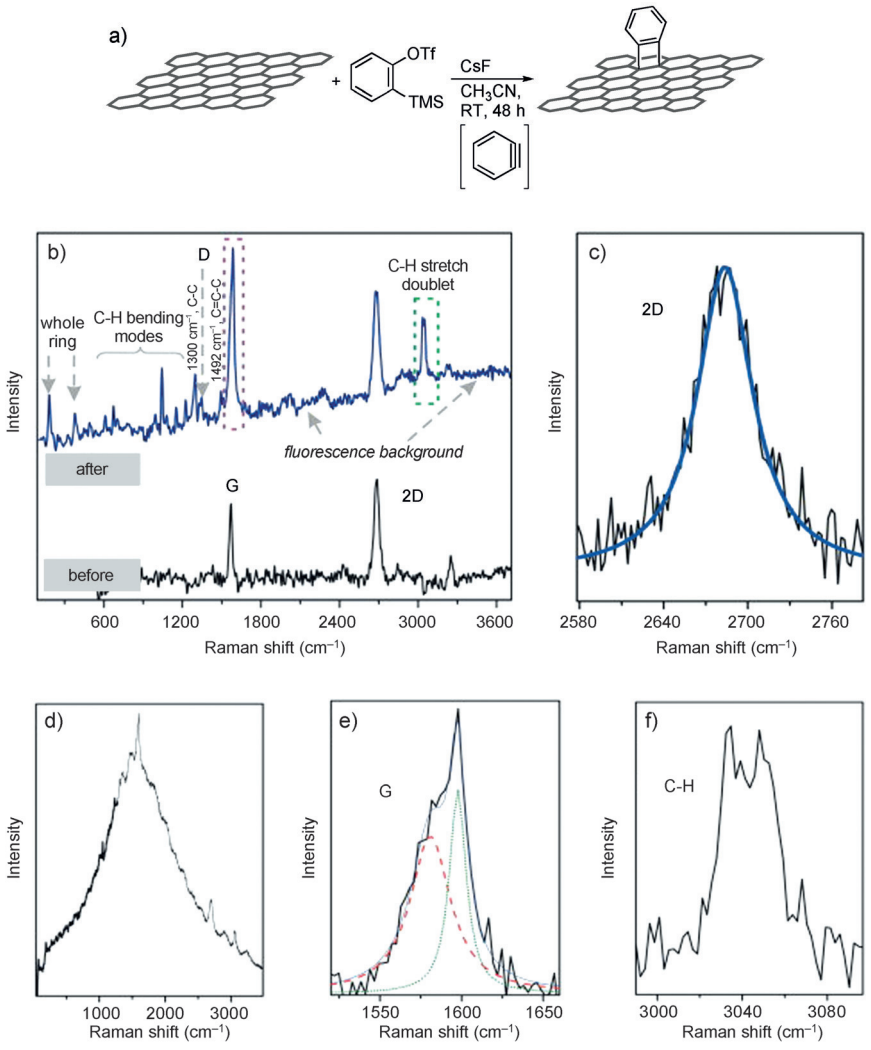

Figure 15. Cycloaddition reaction of Cu/G with benzyne generated from fluoride-induced decomposition of *o*-(trimethylsilyl)phenyl triflate. Raman spectra of Cu/G before (black) and after (blue) benzyne cycloaddition for 8 days. Reproduced from Ref. [64], Copyright 2013 Elsevier.

ure 15b–f). Raman spectra showed direct signals of benzene moieties, such as bands corresponding to C=C–C vibrations (1595 and 1492 cm^{-1}), C–C vibrations (1300 cm^{-1}), C–H stretching and bending at different frequencies. It is worth noting that graphene also generates fluorescence which is visible in the Raman spectrum.

Graphene on substrates has also been functionalized by [2+1] cycloadditions. Although there are different approaches to functionalize graphene by this type of pericyclic reactions,[65] only nitrene addition has been described thus far. Thermally generated nitrene radicals from azidotrimethylsilane have been used to modify SiC/EG under vacuum.[66] Nitrene radicals reacted with the C=C bonds of graphene to form aziridine adducts, creating two adjacent sp^3-hybridized carbon atoms. The degree of functionalization was established by XPS and was relatively low, as shown by the intensity ratio of N/C ≈ 0.019 (Figure 16). In addition, high-resolution photoemission spectroscopy (HRPES) showed the bandgap opening of 0.66 eV, due to the covalent modification.

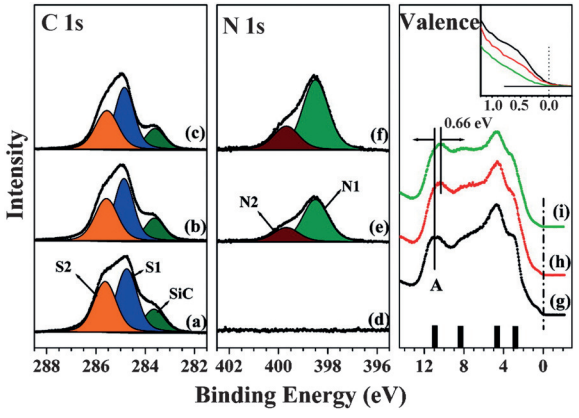

Figure 16. HRPES experiments for graphene functionalization with azidotrimethylsilane: a)–c) C1s core-level spectra obtained at 320 eV, d)–f) N 1s core-level spectra obtained at 500 eV and g)–i) valence band spectra at 130 eV. Samples: SLG (a,d,g); higher (b,e,h) and lower functionalized EG at 100 °C, (c,f,i). Reprinted from Ref. [66], Copyright 2009 American Chemical Society.

Annealing at high temperatures of the functionalized graphene caused the bandgap closure, returning to the intrinsic metallic behavior of graphene.

3.3. Introduction of Single Atoms

Graphene can be covalently modified by attachment of atoms, including hydrogen, fluorine, chlorine, and oxygen. These covalent modifications are very interesting because they are mostly reversible processes and allow for high functionalization levels. Accordingly, semimetal, semiconducting, or insulator materials can be designed. Besides, the functionalized material can be subjected to further covalent functionalization.

3.3.1. Hydrogenation

Hydrogenation of graphene on substrates can be achieved by liquid- and plasma-based processes.[67] The first approach was reported by Geim and Novoselov.[68] Partial hydrogenation of XG on SiO_2/Si was achieved by hydrogen plasma treatment for 2 h, which transforms the highly conductive zero-bandgap semimetal into an insulator. The covalent functionalization was easily reverted by annealing at high temperature (450 °C in Ar atmosphere for 24 h).

Liquid-based methods are the most successful to achieve a high hydrogen

coverage; a well-known example is provided by the Birch reduction.[69] Treatment of single-layer CVD-grown graphene on SiO_2/Si with Li/NH_3 solution, followed by quenching in ethanol, led to hydrogenated graphene, also called graphane, G-H, in just a few seconds. Raman spectroscopy showed a high increase in sp^3 carbon atoms on the graphene structure, with an I_D/I_G ratio of 1.57 and a broadening of all the bands. Additionally, XPS analysis did not exhibit any increase in heteroatom concentration, confirming that no other side reaction had occurred. The drastic hydrogenation produced the elimination of electronic conductivity in the graphene material, transforming it into an insulator with very high resistivity. Besides, Raman spectroscopy and conductivity measurements confirmed the complete reversibility of the process by thermal annealing. Alternatively, when the quenching of the Birch reduction was carried out with tributyltin chloride, a new functionalization of the carbon structure with tributyltin moieties was achieved, as confirmed by XPS analysis.

A high hydrogenation level of a few layers CVDG on SiO_2/Si was also achieved with microwave plasma treatment.[70] In this case, changes in the electronic and magnetic properties were measured as a function of hydrogen introduced in the structure at different substrate temperatures, turning graphene into a room-temperature ferromagnetic semiconductor material. This functionalization opened the possibility of using G-H in spintronic nanodevices, magnetoresistance, or magnetic memory devices.

EG has also been partially hydrogenated.[71] One example is the hydrogenation of Ir (111)/EG for bandgap engineering.[71a] Combined angle-resolved photoemission spectroscopy and STM analysis of EG-H exhibited a bandgap opening that was dependent on H coverage, achieving a gap opening of 73 eV at 23 % of H coverage.

Hydrogenation is a useful strategy for graphene patterning.[72] XG on Si/SiO_2 was coated with hydrogen silsesquioxane (HSQ), and then it was irradiated with an electron beam. This irradiation cleaved Si–H bonds, thereby generating H species that reacted with sp^2 carbon atoms of graphene basal planes. This approach presents high selectivity at room temperature relative to the number of graphene layers. Higher hydrogenation degrees were achieved on SLG relative to BLG. This fact was attributed to the absence of π-stacking on SLG as well as to out-of-plane deformations that stabilize the transition state of the hydrogenation reaction. Besides, the hydrogenation was easily reverted by thermal annealing (100–200 °C). These results enabled the localized generation of reactive species to pave the way toward the reversibly controlled micropatterning of functionalized graphene patches (Figure 17).

Very recently, the dependence between chemical reactivity of supported graphene with the nature of the substrate was also studied in hydrogenation processes.[73] Different supported graphenes based on XG were prepared: SiO_2/SLG, SiO_2/BLG, MoS_2/SLG, and WS_2/SLG, of which the corresponding dichalcogenides are 2D materials. After treatment with HSQ under electron beam irradiation, the SiO_2/SLG showed the highest D-band intensity, whereas SiO_2/BLG, MoS_2/SLG, and WS_2/SLG did not exhibit changes in the D-band. According to the authors, the main reason of the high chemical stability of these graphene substrates formed by 2D structures is the strong van der Waals interaction between the graphene layer and the 2D substrate that hinders geometric lattice deformation of graphene in the reaction.

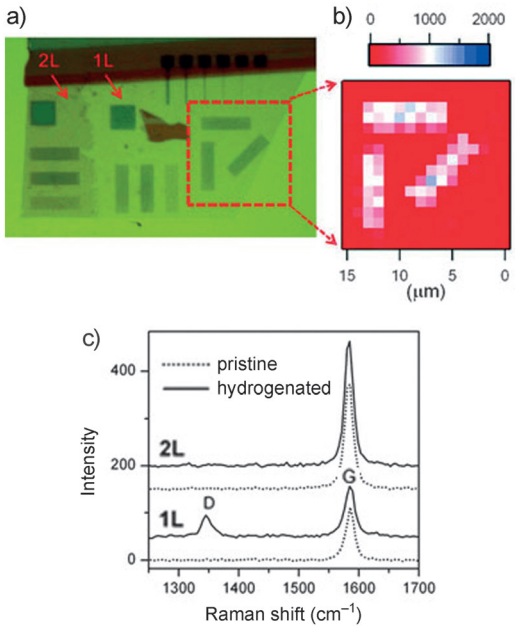

Figure 17. a) Optical image of ebeam-patterned SiO_2/G by hydrogenation. b) D-band Raman map for the squared part in (a). c) Raman spectra of 2 L and 1 L squares in (a). Reproduced from Ref. [72], Copyright 2008 American Chemical Society.

3.3.2. *Halogenation*

Another important class of single-atom attachment is the halogenation reaction. Graphene can be typically halogenated by different methods. This kind of functionalization was only achieved with fluorine or chlorine, due to stability issues with the other halogens. Halogenation of supported graphene can be achieved in a number of ways, for instance, by treatment with halogen-based plasma,[74] by interaction with fluorine atoms derived from the decomposition of fluorinating agents such as XeF_2,[75] and by photochemical reactions.[76] Fluorination is characterized by fast kinetics; therefore, the reaction is difficult to control in terms of functionalization degree.[74e] As a consequence, fluorine attachment resulted in products with wide bandgaps, reduced conductivity, and charge mobility. Moreover, fluorinated graphene can be considered as a viable precursor for the synthesis of other graphene derivatives, as it is susceptible to nucleophilic attacks.[77]

Recently, fluorination of SiC/EG using plasma SF_6 EG has been reported.[74a] The resulting partially fluorinated graphene exhibited F/C ratios of 0.05 and 0.1 from the C-face and the Si-face terminations of SiC, as seen by XPS analysis. By contrast, treatment of SiO_2/CVDG through XeF_2 gas exposure at 30 °C resulted in a highly functionalized material on both sides, with a C_1F_1 stoichiometry; this was possible as the gas is able to pass through the naturally occurring pinholes

underneath the graphene layer, where it preferentially etches silicon and concurrently fluorinates graphene backside.[75a] Analogous treatment of Cu/CVDG led to a single-side functionalized material with C_4F_1 stoichiometry (25 % F coverage). The Raman spectrum of single-side-functionalized graphene exhibited the appearance of a D-signal (1350 cm^{-1}) and the broadening of the graphene band (1580 cm^{-1}), due to the high sp^3 hybridization of carbon atoms. By contrast, functionalization on both sides of graphene cancelled the Raman signals, as a result of the dramatic changes to its structure.

In contrast with fluorination, chlorination exhibits slower kinetics that allow for better control of the functionalization level, without introducing extensive structural damage in the material. For example, Cu/CVDG showed an increase in conductance after plasma treatment with chlorine.[74b] Chlorination of supported graphene led to only partial functionalization with 8 % Cl coverage on SiO_2/G by a photochemical process,[76a] or Au/G-Cl with 8.5 % coverage by a chloride-based plasma.[74e] Very recently, chlorination of single-layer Cu/CVDG was controlled by tuning plasma conditions (Figure 18).[74b] Different functionalization levels were achieved, for which the optimized conditions led to a surface coverage

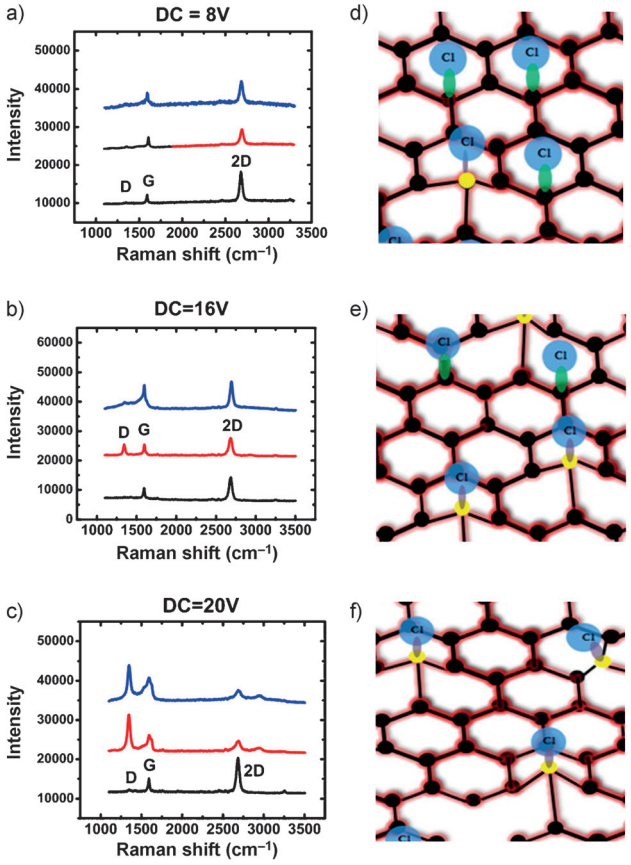

Figure 18. a)–c) Evolution of Raman spectra of Cu/CVDG under different voltages applied in the plasma treatment. Blue: after annealing, red: after chlorination, black: before chlorination. d)–f) Structural representation of Cu/CVDG under different applied voltages. The yellow dots indicate the carbon atoms that experience sp^2-to-sp^3 hybridization change. The purple bonds are covalent C—Cl bonds. The green bonds are ionic bonds between C and Cl. Reprinted from Ref. [74b], Copyright 2013 American Chemical Society.

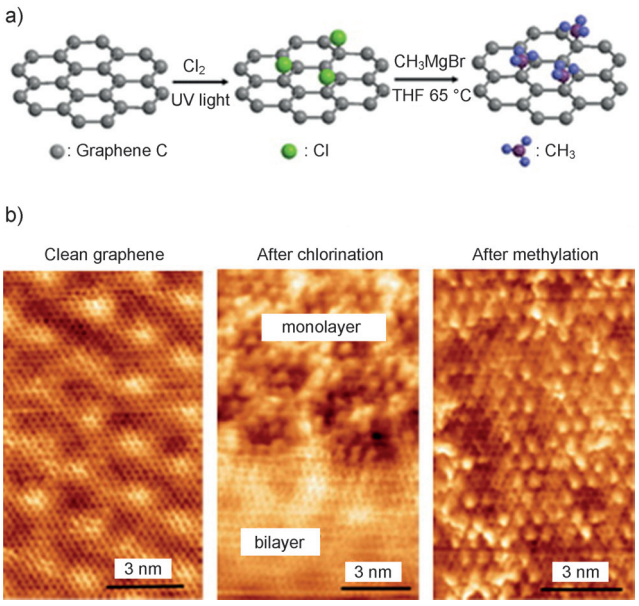

Figure 19. a) Sequential photochlorination and methylation of SiC/EG. b) STM images of SiC/EG in different steps of functionalization. Reprinted from Ref. [76b], Copyright 2012 American Chemical Society.

of 45 % with a good carrier mobility of the G-Cl material. By tuning the plasma conditions, it was also possible to control the interaction between graphene and chlorine atoms (i.e., through ionic bonding, covalent bonding, and defect creation).

Routes to G-Cl are also important as they open the way to the introduction of other molecules by substitution of the Cl, generally a good leaving group. Recently, SiC/EG-Cl was functionalized through nucleophilic substitution with a Grignard reagent (CH_3MgBr, Figure 19).[76b] STM imaging revealed that photochlorination was carried out on the regions where graphene was present as a monolayer. The functionalization with the Grignard reagent was confirmed by the disappearance of Cl peaks and the concomitant increase of the C1s signal in XPS analysis.

3.3.3. Oxidation

Oxidation has traditionally been the most common method in the research community to modify graphene derivatives, to tune their properties, and to explore their functionalization.[13e] Oxidized graphene on a substrate can be easily prepared by aggressive acid treatments starting from graphite, as for example with the Hummers method.[78] However, this material shows inferior electrical conductivity compared to other pristine graphene derivatives. The direct oxidation of EG and CVD-grown graphene overcomes the limitations of GO prepared by Hummers method. Different approaches have been described for oxidizing this kind of graphene derivatives. It is important to consider that during the manufacture of graphene-based devices, the graphene material must be subjected to harsh conditions in the presence of oxygen. For this reason, an understanding of the stability of graphene on substrates under oxygenating conditions is also necessary.

A detailed study of the electrochemical oxidation of EG and its influence on the electronic and optical properties has been reported.[79] Controlled electrochemical oxidation of SiC/EG has been carried out using HNO_3 by applying the corresponding potential. Characterization has been performed by Raman spectroscopy and atomic force microscopy (AFM) at different voltages. The results suggest that the rims in the graphene structures, formed during the synthesis, play an important role in the oxidation process. Probably the curved defects enhance the reactivity in the electrochemical process. The electro-oxidized SiC/EG showed semiconductor behavior with an enhanced photosensitivity relative to pristine EG. Other oxidation methods for EG have been developed, as for example thermal processes. The exposure of SiC/EG to atomic oxygen under ultra-high vacuum conditions generated a covalent homogeneous modification of graphene with oxygenated groups.[80] STM images of oxidized EG showed 1.2 nm-diameter protrusions in the structure, which were interpreted as epoxy groups. In addition, a complete reversibility of the process was observed by thermal annealing at 260 °C as verified by STM, HR-XPS, and Raman spectroscopy. The oxidation degree is clearly tunable by controlling the exposure time against atomic oxygen. Besides, a local oxygen desorption was achieved by applying a high negative voltage through the STM tip. This result might provide a nanopatterning of EG surfaces. Despite being an aggressive type of treatment, supported EG was also treated with the typical Hummers method.[81] The oxidation is strongly dependent on the reaction conditions as previously mentioned. Hersam and co-workers have studied the properties of several oxidized SiC/EG employing two different reaction procedures with Hummers oxidizing agents: either by dipping or drop-casting.[81a] In the first case, SiC/EG was submerged in the corresponding oxidizing aqueous solution, whereas in the second procedure, the oxidizing solution was drop-cast on the substrate and subsequently heated at 60 °C. In both cases, the oxidation led to the same changes in the electronic properties such as an opening of the bandgap (0.4 eV), higher resistivity, and p-type doping. The main difference was observed in the oxygenated groups present in the graphene structure. XPS analysis of dipped-in oxidized SiC/EG showed a heterogeneous material, with a dominant fraction of epoxy groups in addition to carbonyl and hydroxy groups. This oxidation method afforded an oxidized material that could not be reverted back by thermal processes. In contrast, the drop-cast oxidized SiC/EG showed only epoxy groups and could be completely reverted back to pristine EG through annealing at 260 °C. The plasma treatment of SiC/EG in an O_2/Ar led to a covalent modification of the graphene surface by incorporation of oxygen as ether, alcohol, and carboxyl groups, changing its electronic properties.[82] In this instance, the oxidation degree can be controlled by tuning the operating pressure.

The oxidation of CVDG has also been studied to understand its thermal stability in harsh environments.[83] In particular, treatment of single- and bilayer SiO_2/CVDG in air at 550 °C led to structural modifications. For SLG, the disappearance of the typical wrinkles in this kind of graphene and the formation of cracks and pits in the basal plane were already observed after short times of thermal exposure (Figure 20). However, a much higher resistance to the thermal oxidation was found for BLG. The photostability of SiO_2/CVDG has also been studied because it is of major importance for applications under solar radiation.[84] Exposure of SLG to UV/O_3 led to a rapid photooxidation that occurred uniformly on the graphene basal plane. In addition, the process did not produce cracks and pits, in contrast to other oxidation methods.

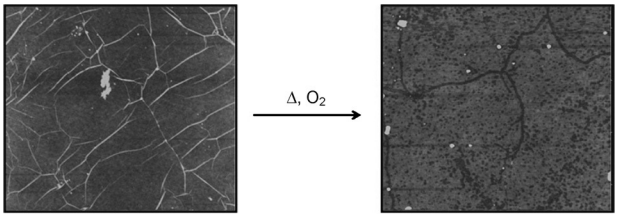

Figure 20. AFM images before (left) and after (right) thermal oxidation at 550 °C of single-layered SiO_2/CVDG. Reprinted from Ref. [83], Copyright 2012 American Chemical Society.

Recent studies of the chemical stability of XG on substrates under oxidizing conditions has also been developed.[73] As we mentioned in Section 3.1, the nature of the substrate is a very important factor in functionalization processes of graphene. UV/O_3 treatment was carried out on SiO_2/SLG and hBN/SLG. Under these conditions, the graphenic structure of SiO_2/SLG was destroyed in a few minutes, whereas in hBN/SLG less defective graphene was detected by Raman spectroscopy, probably due to the stronger van der Waals interactions of graphene and substrate.

4. Conclusions and Outlook

In conclusion, we have discussed the importance of graphene properties (i.e., number of layers, defects, substrate, curvature, etc.) for achieving effective covalent functionalization. This represents an important step forward in the implementation of graphene in practical devices.[85] The unique conducting properties of the graphene structure and its ability to absorb irradiation allow for the use of interesting nonconventional methods for its functionalization,[13b] thereby offering a chance for the development of "green" routes, even in a reversible manner, for applications that require ON/OFF switches or logic states. Electronic devices could be built from the integration of patterned areas of pristine and functionalized graphene that would create metallic or semiconducting regions. This is especially true for functionalization methods that significantly alter the electronic states of graphene, such as stannylation or fluorination as n-doping or p-doping methods, respectively. Alternatively, reversible graphene functionalization could be used to reversibly reduce its conductivity, thus creating 0 and 1 states as two electronic outputs as in logic gates.[86] Implementation of such states with electronic devices could effectively create alternative forms of computing, as is already happening for DNA.[87] Presently, there are still many barriers to overcome in order to realize such great nanotechnological potential. Thermally reversible reactions, such as the Diels–

Alder reaction, require elevated temperatures, which may not be suitable to universal devices. Others, such as fluorination reactions, are often only partially reversible, leaving defects on the graphene structure.[86] Nevertheless, new methods continue to emerge to overcome these limitations. For instance, mechanical stress can drive the cleavage of chemical groups attached on graphene, and the technique is especially successful to remove oxygen and fluorine atoms, as recently shown by AFM.[88]

Covalent modifications of graphene on substrates might also be beneficial for the reliable use of graphene-based devices in demanding biological environments. Many efforts are being made in the field of biotechnology for the development of devices that allow for restoring of damaged abilities.[89] However, there are many challenges for graphene in the field of biotechnology. One of them is the biocompatibility of graphene devices, for which the covalent modification of graphene will be play a fundamental role.

It is therefore apparent that the complete understanding and full control of the functionalization of graphene on substrates has not yet been achieved, leaving a lot of room for further development. In particular, the graphene properties (e.g., surface charge) have been successfully fine-tuned upon covalent modification in solution,[90] and it would be interesting to translate those routes to substrate-supported graphene. In this respect, it is tempting to generally assume higher reactivity for graphene in solution relative to graphene on substrates, as experimentally shown in some cases.[57] However, many examples of innovative methods have been reported to invert the trend and ultimately enhance the reactivity of graphene on substrates (e.g., application of strain[49a] or underlying nanoparticles[42a] to introduce ripples and increase surface curvature, respectively). Many more possibilities exist for graphene on substrates that are just now being unveiled and were simply unthinkable just a few years ago. For instance, graphene could be used as a barrier to mask the underlying substrate from certain chemical reactions, while allowing others, such as acid–base transfers. Indeed, protons can be reversibly transferred from aqueous solutions through natural atomic defects of SLG onto the underlying SiO_2 substrate.[91]

In conclusion, this review should provide readers with some useful tools to make an informed choice amongst the available options to covalently functionalize graphene on substrates (see Table 1). At present, there are still many mechanistic questions that are left unanswered and prevent mastering of the graphene reactivity, but hopefully the current gaps will be of inspiration for new developments in the field of graphene chemistry.

We acknowledge financial support from the University of Trieste, MIUR (FIRB Nanosolar Project, prot. RBAP11C58Y, and Cofin. prot. 2010N3T9M4), the EU FP7-ICT-2013-FET-F GRAPHENE Flagship project (no. 604391). A.C. thanks the Barrié de la Maza Foundation for the award of a research fellowship.

[1] a) K. S. Novoselov, A. K. Geim, S. V. Morozov, D. Jiang, Y. Zhang, S. V. Dubonos, I. V. Grigorieva, A. A. Firsov, *Science* **2004**, *306*, 666 – 669; b) A. K. Geim, K. S. Novoselov, *Nat. Mater.* **2007**, *6*, 183 – 191; c) L. Chen, Y. Hernández, X. Feng, K. Müllen, *Angew. Chem. Int. Ed.* **2012**, *51*, 7640 – 7654; *Angew. Chem.* **2012**, *124*, 7758 – 7773.

[2] P. Wick, A. E. Louw-Gaume, M. Kucki, H. F. Krug, K. Kostarelos, B. Fadeel, K. A. Dawson, A. Salvati, E. Vázquez, L. Ballerini, M. Tretiach, F. Benfenati, E. Flahaut, L. Gauthier, M. Prato, A. Bianco, *Angew. Chem. Int. Ed.* **2014**, *53*, 7714 – 7718; *Angew. Chem.* **2014**, *126*, 7846 – 7850.

[3] a) A. K. Geim, *Science* **2009**, *324*, 1530 – 1534; b) A. H. Castro Neto, N. M. R. Peres, K. S. Novoselov, A. K. Geim, *Rev. Mod. Phys.* **2009**, *81*, 109 – 162; c) A. A. Balandin, *Nat. Mater.* **2011**, *10*, 569 – 581.

[4] S. Wu, Q. He, C. Tan, Y. Wang, H. Zhang, *Small* **2013**, *9*, 1160 – 1172.

[5] a) M. Pumera, *Energy Environ. Sci.* **2011**, *4*, 668 – 674; b) X. Ma, G. Ning, Y. Sun, Y. Pu, J. Gao, *Carbon* **2014**, *79*, 310 – 320.

[6] a) D. S. Su, S. Perathoner, G. Centi, *Chem. Rev.* **2013**, *113*, 5782 – 5816; b) B. F. Machado, P. Serp, *Catal. Sci. Technol.* **2012**, *2*, 54 – 75.

[7] a) Y. Huang, J. Liang, Y. Chen, *Small* **2012**, *8*, 1805 – 1834; b) J. Yun, D. Kim, G. Lee, J. S. Ha, *Carbon* **2014**, *79*, 156 – 164.

[8] a) F. Bonaccorso, Z. Sun, T. Hasan, A. C. Ferrari, *Nat. Photonics* **2010**, *4*, 611 – 622; b) W.-H. Kim, C. S. Park, J. Y. Son, *Carbon* **2014**, *79*, 388 – 392; c) Y.-J. Noh, S.-C. Park, I.-T. Hwang, J.-H. Choi, S.-S. Kim, C.-H. Jung, S.-I. Na, *Carbon* **2014**, *79*, 321 – 329; d) S. Rahimi, L. Tao, S. F. Chowdhury, S. Park, A. Jouvray, S. Buttress, N. Rupesinghe, K. Teo, D. Akinwande, *ACS Nano* **2014**, *8*, 10471 – 10479.

[9] J. M. Tour, *Chem. Mater.* **2014**, *26*, 163 – 171.

[10] a) C. Coletti, C. Riedl, D. S. Lee, B. Krauss, L. Patthey, K. von Klitzing, J. H. Smet, U. Starke, *Phys. Rev. B* **2010**, *81*, 235401; b) T. S. Sreeprasad, V. Berry, *Small* **2013**, *9*, 341 – 350.

[11] S. Giordani, D. Bonifazi, P. Singh, A. Bianco, M. Prato, *Chem. Soc. Rev.* **2009**, *38*, 2214 – 2230.

[12] a) M. Quintana, E. Vazquez, M. Prato, *Acc. Chem. Res.* **2013**, *46*, 138 – 148; b) L. Rodríguez-Pérez, M. Á. Herranz, N. Martín, *Chem. Commun.* **2013**, *49*, 3721 – 3735; c) J. Park, M. Yan, *Acc. Chem. Res.* **2013**, *46*, 181 – 189; d) J. Liu, J. Tang, J. J. Gooding, *J. Mater. Chem.* **2012**, *22*, 12435 – 12452; e) E. Bekyarova, S. Sarkar, S. Niyogi, M. E. Itkis, R. C. Haddon, *J. Phys. D* **2012**, *45*, 154009.

[13] a) S. Eigler, A. Hirsch, *Angew. Chem. Int. Ed.* **2014**, *53*, 7720 – 7738; *Angew. Chem.* **2014**, *126*, 7852 – 7872; b) E. Vázquez, F. Giacalone, M. Prato, *Chem. Soc. Rev.* **2014**, *43*, 58 – 69; c) C. K. Chua, M. Pumera, *Chem. Soc. Rev.* **2013**, *42*, 3222 – 3233; d) V. Georgakilas, M. Otyepka, A. B. Bourlinos, V. Chandra, N. Kim, K. C. Kemp, P. Hobza, R. Zboril, K. S. Kim, *Chem. Rev.* **2012**, *112*, 6156 – 6214; e) D. R. Dreyer, S. Park, W. Bielawski, R. S. Ruoff, *Chem. Rev.* **2010**, *39*, 228 – 240.

[14] F. M. Koehler, W. J. Stark, *Acc. Chem. Res.* **2013**, *46*, 2297 – 2306.

[15] a) A. Ciesielski, P. Samorì, *Chem. Soc. Rev.* **2014**, *43*, 381 – 398; b) M. Cai, D. Thorpe, D. H. Adamson, H. C. Schniepp, *J. Mater. Chem.* **2012**, *22*, 24992 – 25002; c) S. Park, R. S. Ruoff, *Nat. Nanotechnol.* **2009**, *4*, 217 – 224.

[16] Y. I. Zhang, L. Zhang, C. Zhou, *Acc. Chem. Res.* **2013**, *46*, 2329 – 2339.

[17] H. J. Salavagione, *J. Mater. Chem. A* **2014**, *2*, 7138 – 7146.

[18] a) X. Li, W. Cai, J. An, S. Kim, J. Nah, D. Yang, R. Piner, A. Velamakanni, I. Jung, E. Tutuc, S. K. Banerjee, L. Colombo, R. S. Ruoff, *Science* **2014**, *324*, 1312 – 1314; b) S. Bae, H. Kim, Y. Lee, X. Xu, J.-S. Park, Y. Zheng, J. Balakrishnan, T. Lei, H. R.

Kim, Y. I. Song, Y.-J. Kim, K. S. Kim, B. Ozyilmaz, J.-H. Ahn, B. H. Hong, S. Iijima, *Nat. Nanotechnol.* **2010**, *5*, 574 – 578.
[19] R. Piner, H. Li, X. Kong, L. Tao, I. N. Kholmanov, H. Ji, W. H. Lee, J. W. Suk, J. Ye, Y. Hao, S. Chen, C. W. Magnuson, A. F. Ismach, D. Akinwande, R. S. Ruoff, *ACS Nano* **2013**, *7*, 7495 – 7499.
[20] K.-J. Peng, C.-L. Wu, Y.-H. Lin, Y.-J. Liu, D.-P. Tsai, Y.-H. Pai, G.-R. Lin, *J. Mater. Chem. C* **2013**, *1*, 3862 – 3870.
[21] J. Ryu, Y. Kim, D. Won, N. Kim, J. S. Park, E. Lee, D. Cho, S. Cho, S. J. Kim, G. H. Ryu, H. Shin, Z. Lee, *ACS Nano* **2014**, *8*, 950 – 956.
[22] a) S. Sharma, G. Kalita, R. Hirano, S. M. Shinde, R. Papon, *Carbon* **2014**, *72*, 66 – 73; b) B. Hu, H. Ago, Y. Ito, K. Kawahara, M. Tsuji, E. Magome, K. Sumitani, N. Mizuta, K. Ikeda, S. Mizuno, *Carbon* **2012**, *50*, 57 – 65.
[23] a) B. Zhang, W. H. Lee, R. Piner, I. Kholmanov, Y. Wu, H. Li, H. Ji, R. S. Ruoff, *ACS Nano* **2012**, *6*, 2471 – 2476; b) S. Zhu, Q. Li, Q. Chen, W. Liu, X. Li, J. Zhang, Q. Wang, X. Wang, H. Liu, *RSC Adv.* **2014**, *4*, 32941 – 32945.
[24] a) W. Norimatsu, M. Kusunoki, *Phys. Chem. Chem. Phys.* **2014**, *16*, 3501 – 3511; b) K. V. Emtsev, A. Bostwick, K. Horn, J. Jobst, G. L. Kellogg, L. Ley, J. L. McChesney, T. Ohta, S. A. Reshanov, J. Röhrl, E. Rotenberg, A. K. Schmid, D. Waldmann, H. B. Weber, T. Seyller, *Nat. Mater.* **2009**, *8*, 203 – 207.
[25] P. W. Sutter, J.-I. Flege, E. A. Sutter, *Nat. Mater.* **2008**, *7*, 406 – 411.
[26] a) P. Gupta, P. D. Dongare, S. Grover, S. Dubey, H. Mamgain, A. Bhattacharya, M. M. Deshmukh, *Sci. Rep.* **2014**, *4*, 3882/1 – 6; b) S. Unarunotai, J. C. Koepke, C. L. Tsai, F. Du, C. E. Chialvo, Y. Murata, R. Haasch, I. Petrov, N. Mason, M. Shim, J. Lyding, J. A. Rogers, *ACS Nano* **2010**, *4*, 5591 – 5598.
[27] H. Al-Mumen, F. Rao, W. Li, L. Dong, *Nano-Micro Lett.* **2014**, *6*, 116 – 124.
[28] K. S. Kim, Y. Zhao, H. Jang, S. Y. Lee, J. M. Kim, K. S. Kim, J. Ahn, P. Kim, J. Choi, B. H. Hong, *Nature* **2009**, *457*, 706 – 710.
[29] a) K. Parvez, Z. Wu, R. Li, X. Liu, R. Graf, X. Feng, *J. Am. Chem. Soc.* **2014**, *136*, 6083 – 6091; b) J. Wang, K. K. Manga, Q. Bao, K. P. Loh, *J. Am. Chem. Soc.* **2011**, *133*, 8888 – 8891.
[30] a) K. R. Paton, E. Varrla, C. Backes, R. J. Smith, U. Khan, A. O'Neill, C. Boland, M. Lotya, O. M. Istrate, P. King, T. Higgins, S. Barwich, M. Peter, P. Pucz, V. Nico, J. N. Coleman, *Nat. Mater.* **2014**, *13*, 624 – 630; b) J. N. Coleman, *Acc. Chem. Res.* **2013**, *46*, 14 – 22; c) Y. Hernandez, V. Nicolosi, M. Lotya, F. M. Blighe, Z. Sun, S. De, I. T. McGovern, B. Holland, M. Byrne, Y. K. Gun'Ko, J. J. Boland, P. Niraj, G. Duesberg, S. Krishnamurthy, R. Goodhue, J. Hutchison, V. Scardaci, A. C. Ferrari, J. N. Coleman, *Nat. Nanotechnol.* **2008**, *3*, 563 – 568.
[31] C.-J. Shih, A. Vijayaraghavan, R. Krishnan, R. Sharma, J.-H. Han, M.-H. Ham, Z. Jin, S. Lin, G. L. C. Paulus, N. F. Reuel, Q. H. Wang, D. Blankschtein, M. S. Strano, *Nat. Nanotechnol.* **2011**, *6*, 439 – 445.
[32] a) S. Pei, H.-M. Cheng, *Carbon* **2012**, *50*, 3210 – 3228; b) D. C. Marcano, D. V. Kosynkin, J. M. Berlin, A. Sinitskii, Z. Sun, A. Slesarev, L. B. Alemany, W. Lu, J. M. Tour, *ACS Nano* **2010**, *4*, 4806 – 4814.
[33] A. M. Rodriguez, P. Prieto, M. Prato, E. Va, *ACS Nano* **2014**, *8*, 563 – 571.
[34] L.-H. Liu, G. Zorn, D. G. Castner, R. Solanki, M. M. Lerner, M. Yan, *J. Mater. Chem.* **2010**, *20*, 5041 – 5046.
[35] L.-J. Wang, L. Li, J. Yu, Y. Wu, H. He, X. Ouyang, X. Zhao, Y.-C. Yen, L. J. Lee, *Carbon* **2014**, *79*, 294 – 301.
[36] L. Qiu, H. Zhang, W. Wang, Y. Chen, R. Wang, *Appl. Surf. Sci.* **2014**, *319*, 339 – 343.
[37] a) E. Kymakis, K. Savva, M. M. Stylianakis, C. Fotakis, E. Stratakis, *Adv. Funct. Mater.* **2013**, *23*, 2742 – 2749; b) E. Kymakis, E. Stratakis, M. M. Stylianakis, E. Koudoumas, C. Fotakis, *Thin Solid Films* **2011**, *520*, 1238 – 1241.
[38] S.-T. Hsiao, H.-W. Tien, W.-H. Liao, Y.-S. Wang, S.-M. Li, C.-C. Ma, Y.-H. Yu, W.-P. Chuang, *J. Mater. Chem. C* **2014**, *2*, 7284 – 7291.
[39] a) D. W. Boukhvalov, M. I. Katsnelson, *J. Phys. Chem. C* **2009**, *113*, 14176 – 14178; b) S. Park, D. Srivastava, K. Cho, *Nano Lett.* **2003**, *3*, 1273 – 1277.
[40] a) R. C. Haddon, *J. Org. Chem.* **1986**, *108*, 2837 – 2842; b) R. C. Haddon, *J. Org. Chem.* **1987**, *109*, 1676 – 1685; c) R. C. Haddon, *J. Phys. Chem.* **1987**, *91*, 3719 – 3720.
[41] J. C. Meyer, A. K. Geim, M. I. Katsnelson, K. S. Novoselov, T. J. Booth, S. Roth, *Nature* **2007**, *446*, 60 – 63.
[42] a) Q. Wu, Y. Wu, Y. Hao, J. Geng, M. Charlton, S. Chen, Y. Ren, H. Ji, H. Li, D. W. Boukhvalov, R. D. Piner, C. W. Bielawski, R. S. Ruoff, *Chem. Commun.* **2013**, *49*, 677 – 679; b) Y. Cao, K. N. Houk, *J. Mater. Chem.* **2011**, *21*, 1503 – 1508.
[43] D. Jiang, B. G. Sumpter, S. Dai, *J. Phys. Chem. B* **2006**, *110*, 23628 – 23632.
[44] M. Z. Hossain, M. A. Walsh, M. C. Hersam, *J. Am. Chem. Soc.* **2010**, *132*, 15399 – 15403.
[45] J. Pinson, F. Podvorica, J. Pinson, *Chem. Soc. Rev.* **2005**, *34*, 429 – 439.
[46] P. Salice, E. Fabris, C. Sartorio, D. Fenaroli, V. Figà, M. P. Casaletto, S. Cataldo, B. Pignataro, E. Menna, *Carbon* **2014**, *74*, 73 – 82.
[47] a) Q. H. Wang, Z. Jin, K. K. Kim, A. J. Hilmer, G. L. C. Paulus, C.-J. Shih, M.-H. Ham, J. D. Sanchez-Yamagishi, K. Watanabe, T. Taniguchi, J. Kong, P. Jarillo-Herrero, M. S. Strano, *Nat. Chem.* **2012**, *4*, 724 – 732; b) X. Fan, R. Nouchi, K. Tanigaki, *J. Phys. Chem. C* **2011**, *115*, 12960 – 12964.
[48] a) S. Niyogi, E. Bekyarova, M. E. Itkis, H. Zhang, K. Shepperd, J. Hicks, M. Sprinkle, C. Berger, C. N. Lau, W. A. DeHeer, E. H. Conrad, R. C. Haddon, *Nano Lett.* **2010**, *10*, 4061 – 4066; b) R. Sharma, J. H. Baik, C. J. Perera, M. S. Strano, *Nano Lett.* **2010**, *10*, 398 – 405; c) F. M. Koehler, A. Jacobsen, K. Ensslin, C. Stampfer, W. J. Stark, *Small* **2010**, *6*, 1125 – 1130; d) H. Lim, J. S. Lee, H. J. Shin, H. S. Shin, H. C. Choi, *Langmuir* **2010**, *26*, 12278 – 12284.
[49] a) M. A. Bissett, S. Konabe, S. Okada, M. Tsuji, H. Ago, *ACS Nano* **2013**, *7*, 10335 – 10343; b) M. A. Bissett, M. Tsuji, H. Ago, *J. Phys. Chem. C* **2013**, *117*, 3152 – 3159.
[50] L. Gan, D. Zhang, X. Guo, *Small* **2012**, *8*, 1326 – 1330.
[51] H. Liu, S. Ryu, Z. Chen, M. L. Steigerwald, C. Nuckolls, L. E. Brus, *J. Am. Chem. Soc.* **2009**, *131*, 17099 – 17101.
[52] C. K. Chan, T. E. Beechem, T. Ohta, M. T. Brumbach, D. R. Wheeler, K. J. Stevenson, *J. Phys. Chem. C* **2013**, *117*, 12038 – 12044.
[53] S. Sarkar, E. Bekyarova, R. C. Haddon, *Angew. Chem. Int. Ed.* **2012**, *51*, 4901 – 4904; *Angew. Chem.* **2012**, *124*, 4985 – 4988.
[54] M. Steenackers, A. M. Gigler, N. Zhang, F. Deubel, M. Seifert, L. H. Hess, C. H. Y. X. Lim, K. P. Loh, J. A. Garrido, R. Jordan, M. Stutzmann, I. D. Sharp, *J. Am. Chem. Soc.* **2011**, *133*, 10490 – 10498.
[55] L. H. Hess, A. Lyuleeva, B. M. Blaschke, M. Sachsenhauser, M. Seifert, J. A. Garrido, A. Coulombwall, *ACS Appl. Mater. Interfaces* **2014**, *6*, 9705 – 9710.
[56] S. Sarkar, E. Bekyarova, R. C. Haddon, *Acc. Chem. Res.* **2012**, *45*, 673 – 682.
[57] S. Sarkar, E. Bekyarova, S. Niyogi, R. C. Haddon, *J. Am. Chem. Soc.* **2011**, *133*, 3324 – 3327.
[58] S. H. Hoke, J. Molstad, D. Dilettato, M. J. Jay, D. Carlson, B. Kahr, R. G. Cooks, *J. Org. Chem.* **1992**, *57*, 5069 – 5071.
[59] a) A. Criado, M. J. Gómez-Escalonilla, J. L. G. Fierro, A. Urbina, D. Peña, E. Guitián, F. Langa, *Chem. Commun.* **2010**, *46*, 7028 – 7030; b) A. Criado, M. Vizuete, M. J. Gómez-Escalonilla, S. García-Rodriguez, J. L. G. Fierro, A. Cobas, D. Peña, E. Guitián, F. Langa, *Carbon* **2013**, *63*, 140 – 148.

[60] D. Chronopoulos, N. Karousis, T. Ichihashi, M. Yudasaka, S. Iijima, N. Tagmatarchis, *Nanoscale* **2013**, *5*, 6388 – 6394.

[61] X. Zhong, J. Jin, S. Li, Z. Niu, W. Hu, R. Li, J. Ma, *Chem. Commun.* **2010**, *46*, 7340 – 7342.

[62] T. Yang, X. Zhao, S. Nagase, *Org. Lett.* **2013**, *15*, 5960 – 5963.

[63] P. A. Denis, F. Iribarne, *J. Mater. Chem.* **2012**, *22*, 5470 – 5477.

[64] I. V. Magedov, L. V. Frolova, M. Ovezmyradov, D. Bethke, E. A. Shaner, N. G. Kalugin, *Carbon* **2013**, *54*, 192 – 200.

[65] a) M. Naebe, J. Wang, A. Amini, H. Khayyam, N. Hameed, L. H. Li, Y. Chen, B. Fox, *Sci. Rep.* **2014**, *4*, 4375/1 – 7; b) C. Bosch-Navarro, F. Busolo, E. Coronado, Y. Duan, C. Martí-Gastaldo, H. Prima-Garcia, *J. Mater. Chem. C* **2013**, *1*, 4590 – 4598.

[66] J. Choi, K. Kim, B. Kim, H. Lee, S. Kim, *J. Phys. Chem. C* **2009**, *113*, 9433 – 9435.

[67] M. Pumera, C. H. A. Wong, *Chem. Soc. Rev.* **2013**, *42*, 5987 – 5995.

[68] D. C. Elias, R. R. Nair, T. M. G. Mohiuddin, S. V. Morozov, P. Blake, M. P. Halsall, A. C. Ferrari, D. W. Boukhvalov, M. I. Katsnelson, A. K. Geim, K. S. Novoselov, *Science* **2009**, *323*, 610 – 613.

[69] K. E. Whitener, W. K. Lee, P. M. Campbell, J. T. Robinson, P. E. Sheehan, *Carbon* **2014**, *72*, 348 – 353.

[70] S. C. Ray, N. Soin, T. Makgato, C. H. Chuang, W. F. Pong, S. S. Roy, S. K. Ghosh, A. M. Strydom, J. A. McLaughlin, *Sci. Rep.* **2014**, *4*, 3862/1 – 7.

[71] a) R. Balog, B. Jørgensen, L. Nilsson, M. Andersen, E. Rienks, M. Bianchi, M. Fanetti, E. Lægsgaard, A. Baraldi, S. Lizzit, Z. Sljivancanin, F. Besenbacher, B. Hammer, T. G. Pedersen, P. Hofmann, L. Hornekær, *Nat. Mater.* **2010**, *9*, 315 – 319; b) N. P. Guisinger, G. M. Rutter, J. N. Crain, P. N. First, J. A. Stroscio, *Nano Lett.* **2009**, *9*, 1462 – 1466.

[72] S. Ryu, M. Y. Han, J. Maultzsch, T. F. Heinz, P. Kim, M. L. Steigerwald, L. E. Brus, *Nano Lett.* **2008**, *8*, 4597 – 4602.

[73] J. H. Lee, A. Avsar, J. Jung, J. Y. Tan, K. Watanabe, T. Taniguchi, S. Natarajan, G. Eda, S. Adam, A. H. Castro Neto, B. Özyilmaz, *Nano Lett.* **2014**, *15*, 319 – 325.

[74] a) S. Zhou, S. D. Sherpa, D. W. Hess, A. Bongiorno, *J. Phys. Chem. C* **2014**, *118*, 26402 – 26408; b) X. Zhang, A. Hsu, H. Wang, Y. Song, J. Kong, M. S. Dresselhaus, T. Palacios, *ACS Nano* **2013**, *7*, 7262 – 7270; c) B. Wang, J. Wang, J. Zhu, W. E. T. Al, *ACS Macro Let.* **2014**, *8*, 1862 – 1870; d) M. Ghazinejad, J. Reiber Kyle, S. Guo, D. Pleskot, D. Bao, V. I. Vullev, M. Ozkan, C. S. Ozkan, *Adv. Funct. Mater.* **2012**, *22*, 4519 – 4525; e) J. Wu, L. Xie, Y. Li, H. Wang, Y. Ouyang, J. Guo, H. Dai, *J. Am. Chem. Soc.* **2011**, *133*, 19668 – 19671.

[75] a) J. T. Robinson, J. S. Burgess, C. E. Junkermeier, S. C. Badescu, T. L. Reinecke, F. K. Perkins, M. K. Zalalutdniov, J. W. Baldwin, J. C. Culbertson, P. E. Sheehan, E. S. Snow, *Nano Lett.* **2010**, *10*, 3001 – 3005; b) Q. Li, X.-Z. Liu, S.-P. Kim, V. B. Shenoy, P. E. Sheehan, J. T. Robinson, R. W. Carpick, *Nano Lett.* **2014**, *14*, 5212 – 5217; c) V. Wheeler, N. Garces, L. Nyakiti, R. Myers-Ward, G. Jernigan, J. Culbertson, C. Eddy, K. D. Gaskill, *Carbon* **2012**, *50*, 2307 – 2314; d) R. R. Nair, W. Ren, R. Jalil, I. Riaz, V. G. Kravets, L. Britnell, P. Blake, F. Schedin, A. S. Mayorov, S. Yuan, M. I. Katsnelson, H.-M. Cheng, W. Strupinski, L. G. Bulusheva, A. V. Okotrub, I. V. Grigorieva, A. N. Grigorenko, K. S. Novoselov, A. K. Geim, *Small* **2010**, *6*, 2877 – 2884.

[76] a) B. Li, L. Zhou, D. Wu, H. Peng, K. Yan, Y. Zhou, Z. Liu, *ACS Nano* **2011**, *5*, 5957 – 5961; b) S. Yoshimoto, K. Mukai, T. Koitaya, J. Yoshinobu, S. Hosaka, *J. Phys. Chem. C* **2014**, *118*, 22096 – 22101.

[77] M. Dubecký, E. Otyepková, P. Lazar, F. Karlický, M. Petr, K. Čépe, P. BanáŠ, R. Zbořil, M. Otyepka, *J. Phys. Chem. Lett.* **2015**, *6*, 1430 – 1434.

[78] W. S. Hummers, R. E. Offeman, *J. Am. Chem. Soc.* **1958**, *80*, 1339 – 1339.

[79] M. E. Itkis, F. Wang, P. Ramesh, E. Bekyarova, S. Niyogi, X. Chi, C. Berger, W. A. de Heer, R. C. Haddon, *Appl. Phys. Lett.* **2011**, *98*, 093115.

[80] M. Z. Hossain, J. E. Johns, K. H. Bevan, H. J. Karmel, Y. T. Liang, S. Yoshimoto, K. Mukai, T. Koitaya, J. Yoshinobu, M. Kawai, A. M. Lear, L. L. Kesmodel, S. L. Tait, M. C. Hersam, *Nat. Chem.* **2012**, *4*, 305 – 309.

[81] a) J. Yoshinobu, H. Sone, S. Hosaka, M. C. Hersam, *J. Phys. Chem. C* **2014**, *118*, 1014 – 1020; b) S. Kim, S. Zhou, Y. Hu, M. Acik, Y. J. Chabal, C. Berger, W. de Heer, A. Bongiorno, E. Riedo, *Nat. Mater.* **2012**, *11*, 544 – 549.

[82] S. C. Hernández, V. D. Wheeler, M. S. Osofsky, G. G. Jernigan, V. K. Nagareddy, A. Nath, E. H. Lock, L. O. Nyakiti, R. L. Myers-Ward, K. Sridhara, A. B. Horsfall, C. R. Eddy, D. K. Gaskill, S. G. Walton, *Surf. Coat. Technol.* **2014**, *241*, 8 – 12.

[83] S. P. Surwade, Z. Li, H. Liu, *J. Phys. Chem. C* **2012**, *116*, 20600 – 20606.

[84] S. Zhao, S. P. Surwade, Z. Li, H. Liu, *Nanotechnology* **2012**, *23*, 355703.

[85] A. C. Ferrari, F. Bonaccorso, V. Fal′ko, K. S. Novoselov, S. Roche, P. Bøggild, S. Borini, F. H. L. Koppens, V. Palermo, N. Pugno, J. A. Garrido, R. Sordan, A. Bianco, L. Ballerini, M. Prato, E. Lidorikis, J. Kivioja, C. Marinelli, T. Ryhänen, A. Morpurgo, J. N. Coleman, V. Nicolosi, L. Colombo, A. Fert, M. Garcia-Hernandez, A. Bachtold, G. F. Schneider, F. Guinea, C. Dekker, M. Barbone, Z. Sun, C. Galiotis, A. N. Grigorenko, G. Konstantatos, A. Kis, M. Katsnelson, L. Vandersypen, A. Loiseau, V. Morandi, D. Neumaier, E. Treossi, V. Pellegrini, M. Polini, A. Tredicucci, G. M. Williams, B. H. Hong, J.-H. Ahn, J. M. Kim, H. Zirath, B. J. VanWees, H. van der Zant, L. Occhipinti, A. Di Matteo, I. A. Kinloch, T. Seyller, E. Quesnel, X. Feng, K. Teo, N. Rupesinghe, P. Hakonen, S. R. T. Neil, Q. Tannock, T. Löfwanderaq, J. Kinaretba, *Nanoscale* **2015**, *7*, 4598 – 4810.

[86] K. E. Whitener, Jr., in *The Science and Function of Nanomaterials: From Synthesis to Application*, ACS Symposium Series, American Chemical Society, Washington, **2014**, Chap. 3, pp. 41 – 54.

[87] H. Li, Y. Liu, S. Dong, E. Wang, *NPG Asia Mater.* **2015**, *7*, e166 – e168.

[88] K. E. W. Jr, J. T. Robinson, J. R. Felts, A. J. Oyer, S. C. Herna, S. G. Walton, P. E. Sheehan, *Nat. Commun.* **2015**, *6*, 6467/1 – 7.

[89] B. L. H. Hess, M. Seifert, J. A. Garrido, *Proc. IEEE* **2013**, *101*, 1780 – 1792.

[90] a) C. Hadad, X. Ke, M. Carraro, A. Sartorel, C. Bittencourt, G. Van Tendeloo, M. Bonchio, M. Quintana, M. Prato, *Chem. Commun.* **2014**, *50*, 885 – 887; b) X. Ke, S. Turner, M. Quintana, C. Hadad, A. Montellano-López, M. Carraro, A. Sartorel, M. Bonchio, M. Prato, C. Bittencourt, G. Van Tendeloo, *Small* **2013**, *9*, 3922 – 3927; c) M. Quintana, A. M. López, S. Rapino, F. M. Toma, M. Iurlo, M. Carraro, A. Sartorel, C. MacCato, X. Ke, C. Bittencourt, T. Da Ros, G. Van Tendeloo, M. Marcaccio, F. Paolucci, M. Prato, M. Bonchio, *ACS Nano* **2013**, *7*, 811 – 817; d) M. Quintana, K. Spyrou, M. Grzelczak, W. R. Browne, P. Rudolf, M. Prato, *ACS Nano* **2010**, *4*, 3527 – 3533.

[91] J. L. Achtyl, R. R. Unocic, L. Xu, Y. Cai, M. Raju, W. Zhang, R. L. Sacci, I. V. Vlassiouk, P. F. Fulvio, P. Ganesh, D. J. Wesolowski, S. Dai, A. C. T. Van Duin, M. Neurock, F. M. Geiger, *Nat. Commun.* **2015**, *6*, 6539/1 – 7.